Activation of the NFκB pathway alters the phenotype of MSCs in the tracheal aspirates of preterm infants with severe BPD

Tobias Reicherzer[1,2], Susanne Häffner[1,2], Tayyab Shahzad[3], Judith Gronbach[3], Josef Mysliwietz[4], Christoph Hübener[5], Uwe Hasbargen[5], Jan Gertheiss[6], Andreas Schulze[1], Saverio Bellusci[7], Rory E. Morty[8], Anne Hilgendorff[1,2], and Harald Ehrhardt[1,3]

[1] Division of Neonatology, University Children's Hospital, Perinatal Center, Ludwig-Maximilians-University, Campus Großhadern, Marchioninistr.15, Munich D-81377, Germany

[2] Comprehensive Pneumology Center, Ludwig-Maximilians-University, Asklepios Hospital, and Helmholtz Center Munich, Max-Lebsche Platz 31, 81377 Munich, Germany

[3] Department of General Pediatrics and Neonatology, Justus-Liebig-University and Universities of Giessen and Marburg Lung Center (UGMLC), Feulgenstrasse 12, D-35392 Gießen, Member of the German Lung Research Center (DZL)

[4] Institute of Molecular Immunology, Helmholtz Center Munich, Marchioninistrasse 25, D-81377 Munich, Germany

[5] Department of Obstetrics and Gynecology, Perinatal Center, University Hospital, Ludwig-Maximilians-University, Marchioninistrasse 15, D-81377 Munich, Germany

[6] Institute of Applied Stochastics and Operations Research, Research Group Applied Statistics, Clausthal University of Technology, Erzstrasse 1, D-38678 Clausthal-Zellerfeld, Germany

[7] Universities of Giessen and Marburg Lung Center (UGMLC), Excellence Cluster Cardio-Pulmonary System (ECCPS), Member of the German Center

for Lung Research (DZL), Department of Internal Medicine II, Aulweg 130, 35392, Giessen, Germany

[8] Department of Lung Development and Remodeling, Max Planck Institute for Heart and Lung Research, Member of the German Lung Center (DZL), 61231, Bad Nauheim, Germany

Author contributions: TR, SH, TS, JG, JM, and HE conceived and performed the experiments. JG, TR, and HE analyzed data and generated figures. CH, UH, AS, and HE collected data and enrolled patients. HE and TR wrote the manuscript and researched the literature. AH, SB, and REM provided critical insights and intellectual contributions to the manuscript. All authors have approved the submitted manuscript.

Running head: Mesenchymal stromal cells and bronchopulmonary dysplasia

Corresponding author:

Harald Ehrhardt

Department of General Pediatrics and Neonatology

Justus-Liebig-University

Feulgenstrasse 12, D-35392 Gießen

tel. +49 985 43400, fax +49 985 43419

Harald.Ehrhardt@paediat.med.uni-giessen.de

Abstract

Mesenchymal stromal cells (MSCs) are released into the airways of preterm infants following lung injury. These cells display a pro-inflammatory phenotype and are associated with development of severe bronchopulmonary dysplasia (BPD). We aimed to characterize the functional properties of MSCs obtained from tracheal aspirates of 50 preterm infants who required invasive ventilation. Samples were separated by disease severity. The increased proliferative capacity of MSCs was associated with longer duration of mechanical ventilation and higher severity of BPD. Augmented growth depended on nuclear accumulation of NFκBp65 and was accompanied by reduced expression of cytosolic α-SMA. The central role of NFκB signaling was confirmed by inhibition of IκBα phosphorylation. The combined score of proliferative capacity, accumulation of NFκBp65, and expression of α-SMA were used to predict the development of severe BPD with an area under the curve (AUC) of 0.847. We mimicked the clinical situation *in vitro*, and stimulated MSCs with IL-1β and TNF-α. Both cytokines induced similar and persistent changes as was observed in MSCs obtained from preterm infants with severe BPD. RNA interference was employed to investigate the mechanistic link between NFκBp65 accumulation and alterations in phenotype. Our data indicate that determining the phenotype of resident pulmonary MSCs represents a promising biomarker-based approach. The persistent alterations in phenotype, observed in MSCs from preterm infants with severe BPD, were induced by the pulmonary inflammatory response. NFκBp65 accumulation was identified as a central regulatory mechanism. Future preclinical and clinical studies, aimed to prevent BPD, should focus on phenotype changes in pulmonary MSCs.

Keywords NFκB; αSMA; preterm; mesenchymal stromal cells; bronchopulmonary dysplasia

Introduction

Bronchopulmonary dysplasia (BPD) is caused by injury to the developing lung, leading to life-long sequelae (14, 20). Histopathology of BPD shows simplified alveolar structures and dysmorphic capillary configuration (7). The disturbance of lung development and severity of BPD are caused by perinatal and postnatal factors, including prematurity, genetic susceptibility, prenatal and postnatal infections, mechanical ventilation, and oxygen toxicity. These factors cause a pulmonary inflammatory response that is central to the pathogenesis of BPD. BPD is characterized by an imbalance between pro- and anti-inflammatory cytokines, downregulation of vascular and tissue growth factors, influx of inflammatory cells, formation of reactive oxygen species and activation of proteases (17, 43).

The transcription factor NFκB is essential for normal lung development, but excessive signaling during pulmonary inflammation is a critical mechanism in abnormal lung development (15, 19, 27, 41). In line with this, the accumulation of pro-inflammatory cytokines, such as IL-1β or TNF-α, which activate NFκB, perturbs normal lung development. Conversely, mechanical ventilation in an oxygen-rich environment can also lead to increased lung damage when NFκB signaling and levels of TNF-α are reduced (4, 11). Therefore, therapeutic targeting of NFκB signaling needs to be critically re-evaluated.

In recent years, pioneering studies have focused on MSCs obtained from the tracheal aspirates of ventilated preterm infants. These cells fulfilled the classical criteria of MSCs and displayed a lung-specific phenotype, which distinguished them from non-resident MSCs (3, 8, 9, 16, 29, 39). Isolation of MSCs from tracheal aspirates of ventilated preterm infants in these studies was particularly successful from tracheal aspirates of infants who later developed BPD. This finding led to the conclusion that the release of MSCs into the airway is the result of lung injury. These MSCs

106 demonstrated substantial alterations in the pathways controlled by PDGF receptor α,
107 β-catenin, and TGF-β1, which regulate the differentiation of MSCs into
108 myofibroblasts. These alterations were associated with distortion of further septation
109 and interstitial fibrosis (16, 29, 33, 37, 38, 40).
110 We performed detailed descriptive, functional, and molecular studies on MSCs
111 obtained from the tracheal aspirates of preterm infants. We identified a combination
112 of new phenotypic characteristics predictive of a prolonged need for mechanical
113 ventilation and higher severity of BPD. Finally, we mimicked the effects of an
114 inflammatory milieu *in vivo* by exposing MSCs to pro-inflammatory cytokines *in vitro*.
115 This induced phenotype alterations similar to those observed in MSCs isolated from
116 preterm infants with severe BPD.
117

Materials and Methods

For flow cytometry, the antibodies anti-CD45 (1:50, MHCD4518), anti-CD13 (1:50, MHCD1301), anti-CD105 (1:50, MHCD10505), anti-CD34 (1:50, CD34-581-18), and anti-CD14 (1:50, MHCD1427) were obtained from Caltag (Towcester, UK); anti-CD73 (1:50, 550257), anti-CD90 (1:50, 559869), anti-CD11b (1:50, 557743), and anti-CXCR4 (1:50, 555974) were obtained from BD Biosciences (San Diego, CA, USA). Isotype control antibodies were obtained from BD Biosciences. For western blotting, the antibodies anti-Histone H1 (1:500, sc-10806), anti-Lamin A/C (1:1000, sc-6214), and anti-NFκBp65 (1:500, sc-372) were obtained from Santa Cruz (Santa Cruz, CA, USA); anti-α-SMA (1:1000, 113200) was obtained from Calbiochem (San Diego, CA, USA), anti-p-IκBα (1:1000, 2859) and anti-IκBα (1:1000, 9242) were obtained from Cell Signaling Technology (Danvers, MA), anti-GAPDH (1:2500, MA1-22670) and fluorochrome-conjugated secondary antibodies were obtained from Thermo Fisher (Waltham, MA). Cytokines were obtained from PeproTech (Hamburg, Germany). All other reagents were obtained from Sigma-Aldrich (Munich, Germany). All antibodies used in the manuscript can be found in SciCrunch database.

Study cohort, cell culture, and study parameters

A cohort of 112 preterm infants (<29 weeks of gestational age) from the PROTECT (PROgress in the molecular understanding of The evolution of Chronic lung disease in premature infants Trial) study was eligible for this study. Of these patients, five were excluded because of fungal or bacterial cell culture contamination. No child was excluded because of insufficient sampling. A total of 50 preterm infants met the evaluation criteria of i) mechanical ventilation for ≥7 days and ii) routine suctioning performed at least every other day until successful establishment of MSC cultures. Chorioamnionitis was proven by histopathologic examination. All experiments were

approved by the ethics committees of the Ludwig-Maximilians-University Munich (#195-07) and the Justus-Liebig-University Gießen (#135/12). All MSC samples subjected to cohort analyses were collected at the Munich site. No changes in the ventilation strategies were introduced into the clinical routine during the study period. All procedures involving human subjects were in accordance with the principles of the Helsinki Declaration. Written informed consent was obtained from the parents of all infants.

Preservation of primary samples, cell culture, transfection experiments, and experimental readouts

Cell culture

Cell pellets from tracheal aspirates were resuspended in MesenCult medium supplemented with 20% fetal calf serum (FCS; Stemcell Technologies, Vancouver, Canada), 2 mM L-glutamine, 10 mM HEPES buffer solution, 50 U/ml penicillin, 50 µg/ml streptomycin, and 50 µg/ml gentamicin (Invitrogen, Carlsbad, CA, USA). MSCs were allowed to grow to confluence. Established cultures were maintained under constant growth. The purity of >95% of MSC cultures was determined by cell-surface staining assay described below (3, 16, 33, 39). Experiments were conducted between passages 2−6 in DMEM medium (PAN Biotech GmbH, Aidenbach, Germany) without FCS. The area of the well, covered by cells at the start of experiments, ranged between 10 and 25%.

Cell transfection

Transient transfection was performed with Lipofectamine 2000 (Life Technologies) according to the manufacturer's instructions. siRNA against NFκBp65 (5'-GCCCUAUCCCUUUACGUCA -3' (MWG Biotech, Ebersberg, Germany) and AllStars negative control siRNA (Qiagen, Hilden, Germany) was used at a concentration of 20

nM. Experiments were started 24 hours after transfection. Iκκ2 inhibitor IV (Merck KGaA) was used to inhibit the phosphorylation of IκBα.

Flow cytometry

The induction of apoptosis was determined using Nicoletti staining (32). For multicolor flow cytometry, cells were washed in a buffer containing 2% glucose, 1% BSA, 0.1% EDTA, and 0.1% sodium azide. Cells were resuspended and incubated with fluorochrome-conjugated antibodies at a concentration of 1:50. We used four different antibody panels: one containing CD13-FITC, CD73-PE, CD34-PerCP-Cy5.5, and CD14-APC-Cy7; one containing CD105-PE, CD45-PerCP-Cy5.5, CD14-APC-Cy7, and CD90-APC; one with CD45-PerCP-Cy5.5, CD90-APC, and CD14-APC-Cy7; and one containing CD95-FITC, CXCR4-PE, and CD11b-PECy7. Propidium iodide (1 µg/ml) was added to each panel to label and sort out dead cells. Negative controls were stained with an isotype control panel. Flow cytometry was performed using an LSR II device. Facs Diva software version 6.1.3 (BD Biosciences) was used for data acquisition, and FlowJo analysis-software version 8.8.6 (Tree Star Inc., Ashland, VA, USA) was used for analyses. Compensation was performed with leftover cells and compensation beads (BD Biosciences).

Cell proliferation assays

For quantification of cell proliferation, cells were plated in a 96-well plate, with density defined as 10 to 25% of the well area covered. The change in the well area covered was observed over time using a Cellscreen device and data acquisition using PA adhesion software (Innovatis AG, Bielefeld, Germany). Manual cell counts were performed in a Neubauer chamber after the addition of trypan blue.

Western blot analysis

Cytosolic extracts were obtained by cell lysis in 10 mM 4-(2-hydroxyethyl)-1-piperazineethanesulfonic acid (HEPES, pH 7.0), 1 mM KCl, 1.5 mM $MgCl_2$, and 0.5% Triton-X supplemented with a proteinase inhibitor cocktail I (Merck KGaA). Nuclear extracts were obtained after lysis of cell nuclei in 20 mM HEPES (pH 7.9), 400 mM KCl, 0.1 mM EDTA, and 25% glycerin. Protein density was quantified using AIDA imaging software version 2.50 (Raytest, Straubenhardt, Germany). An internal standard deposited on each gel enabled the comparison between different gels.

Histological staining and immunofluorescence

Cells were incubated for 9−18 days in a medium containing dexamethasone (10 µmol), isobutylmethylxanthine (100 µg/ml), indomethacin (50 µmol), and insulin (10 µg/ml, Sanofi-Aventis, Frankfurt, Germany) for adipocyte differentiation, and in a medium containing dexamethasone (0.1 µmol), β-glycerophosphate (10 mmol), and L-ascorbic-acid (50 µg/ml) for osteoblast differentiation. Culture medium was exchanged every third day. For myofibroblast differentiation, cells were incubated with 1 ng/ml TGFβ added to the medium for 48 hours (16, 36).

Histological detection of adipocytic and osteoblastic differentiation was conducted with Oil Red O or Alizarin Red staining, respectively. Immunofluorescence was performed using sterilized glass slides. Cells were fixed either in methanol or acetone, permeabilized with Triton-X, rinsed in phosphate-buffered saline (PBS), and stained with specific primary antibodies and fluorochrome-conjugated secondary antibodies. Cells were then mounted on slides, and the nuclei were counterstained using Vectashield mounting medium with DAPI (Vector Labs, Burlingame, CA, USA). Images were acquired using a Zeiss Axiovert 200 M fluorescent microscope (Zeiss, Jena, Germany) and OpenLab software version 3.0.8 (Improvision, Coventry, UK).

221 **Determination of cytokine levels in tracheal aspirates**

222 Protein expression of IL-1β was measured in tracheal aspirates using the IL-1β
223 Quantikine ELISA kit (R&D Systems, Minneapolis, MN) according to the
224 manufacturer's instructions. Standardization to sIgA (Immunodiagnostik AG,
225 Bensheim, Germany) was performed to compensate for the dilution effects of the
226 suctioning procedures (11).

227

228 **Statistical analysis**

229 The proliferation index (PI) was calculated as the quotient of [well area covered at the
230 end of the experiment / well area covered at the start of the experiment].
231 Student's *t*-test was used to test for statistically significant differences between two
232 independent groups. Multivariate analyses were performed using an analysis of
233 variance (ANOVA) test, and Bonferroni correction was used to adjust for multiple
234 comparisons. Association studies were analyzed with Spearman's rank order
235 correlation coefficient, and regression analyses were performed with a standard
236 linear logistic model or a proportional odds model, depending on the type of the
237 response variable (metric/binary/ordinal). We used a linear mixed model with random
238 intercept to test for effects on batches of MSC cultures obtained from different
239 children. A child-specific random intercept was included to account for dependencies
240 between observations of the same child. Differences were considered statistically
241 significant at p-values <0.05.

242

243

Results

We performed an observational study of a prospective cohort of 112 preterm infants (<29 weeks of gestation), and determined the phenotype of MSCs isolated from the tracheal aspirates of these infants. Patient characteristics are described in Table 1.

Presence and characterization of MSCs

MSCs were detected in the tracheal aspirates of every preterm infant ventilated for at least the first 7 days of life (data not shown). Cells grew to confluence within 8−16 days. Standardized protocols (depicted in Figure 1A) were started at passage 2. Flow cytometric analyses confirmed the specific phenotype of MSCs and the high purity of cultured cells (9, 16, 33). MSCs were identified by flow cytometry. MSCs were positive for MSC surface markers CD13, CD73, CD90, and CD105 and negative for CD11b, CD14, CD34, CD45, and CXCR4; CD11b, CD14, CD34, CD45, and CXCR4 are markers of hematopoietic precursors, leukocytes, macrophages, dendritic cells, fibrocytes, and endothelial cells and are not expressed on MSCs (Figure 1B) (9, 16, 26, 31, 34, 44). The characteristic pluripotency of MSCs was confirmed by adipocytic, osteoblastic, and myofibroblastic differentiation (Figure 1C). Stability of cell characteristics was assured until passage 6 by testing the relevant phenotypic parameters (Figure 1D).

Because 49 of the 50 infants fulfilled the criteria for having BPD, we focused on the degrees of BPD severity (Table 1) (21). Neither the day of first appearance nor the duration of successful cultivation from tracheal aspirates was predictive for the severity of BPD (Figure 2 and Table 2). As expected, children with high severity of BPD needed prolonged ventilatory support. There was no difference in the distribution of BPD severity between preterm infants with MSC present in tracheal

aspirates within the first seven days of life and those with MSC present in tracheal aspirates only after day 7 and before day 21 of life (Table 3).

These data are in agreement with previous observations showing that the presence of MSCs is associated with the development of BPD (3, 16, 39). Therefore, we then evaluated characteristics that could be used to discriminate among MSCs derived from children with better and poorer pulmonary outcomes.

Proliferative capacity of MSCs as a predictor of the duration of mechanical ventilation and severity of BPD

MSCs were grouped according to disease severity into mild, moderate, and severe BPD. MSCs from the three groups did not differ in the density of surface receptor expression and potential for adipogenic, osteogenic, or myofibroblastic differentiation (data not shown). The duration for establishing a successful MSC culture at passage 0 varied highly among the cells obtained from different patients. This observation was reproduced under standardized conditions in cell culture. Automated repetitive light microscopy was used to determine the changes in well area covered over time (Figure 3A). The proliferation index (PI) was introduced to compensate for differences in the well area covered at the start of the experimental procedures (Figure 3B). Automated repetitive light microscopy (Figure 3C) and manual cell counting (Figure 3D) yielded identical results in selected experiments and indicated that the increase in the well area covered resulted from an increase in absolute cell numbers. Using Nicoletti staining, we ruled out the notion that the difference in absolute cell numbers was a consequence of variations in cell death (Figure 3E). When MSC samples were separated by disease severity, statistically significant differences in the PI were observed between the groups (Figure 4A). Using a proportional odds model and logistic regression, followed by inspection of the receiver operating characteristic

(ROC) curve, the PI was predictive of BPD-severity (Figure 4B and data not shown). In agreement with this result, a higher PI was associated with longer duration of ventilatory support. The PI was not impacted by early or late time points of first establishing the MSC culture (Figure 4C and Tables 2 and 3).

Thus, the severity of BPD can be predicted from alterations in the proliferative capacity of MSCs.

Proliferative capacity of MSCs is correlated with accumulation of NFκBp65 and downregulation of α-SMA

The earliest changes, observed in the lungs of preterm infants who later developed BPD, included the influx of inflammatory cells and an imbalance of inflammatory cytokines and growth factors. Because NFκB is a central regulator of most inflammatory processes and proliferation (15, 41), we focused on the contribution of NFκB to heterogeneous growth characteristics. MSC samples that displayed a particularly low or high PI were selected and assayed for nuclear accumulation of NFκBp65. Western blotting revealed clear differences in the levels of NFκBp65 (Figure 5A). Next, MSCs from the entire cohort were assayed for the expression of NFκBp65 with the help of computer-based image quantification (Figure 5B). Separating samples by disease severity revealed a significant difference in nuclear accumulation of NFκBp65 among samples of MSCs from preterm infants with mild and severe BPD (Figure 5C). Applying the proportional odds model revealed that high levels of NFκBp65 were predictive for the development of severe BPD (Figure 5D). Biochemical inhibition of the phosphorylation of IκBα confirmed that NFκB signaling is important for controlling proliferation in MSCs (Figure 5E).

Next, we studied additional intracellular markers to detect correlations with the development of severe BPD. We assessed proteins typically expressed in mesenchymal cells including α-SMA, Collagen Iα, myosin heavy chain, and PDGFR-α. Only the levels of α-SMA differed among the three groups (Figure 6A). MSC samples revealed an inverse cytosolic expression level of α-SMA and nuclear NFκBp65 (Figure 6B). As observed for the expression of PI and NFκBp65, the expression level of α-SMA was distinctly correlated with the degree of BPD severity (Figure 6C). A high expression level of α-SMA was predictive of a good pulmonary outcome (Figure 6D). The combined analysis of the levels of PI, NFκBp65, and α-SMA revealed good accuracy of prediction for moderate or severe BPD when logistic regression was used with an area under the curve (AUC) of 0.847 (Figure 6E).

Taken together, the parameters PI, NFκBp65 accumulation, and expression of α-SMA are useful markers to predict the pulmonary prognosis.

Regulation of proliferative capacity of MSCs and α-SMA expression by NFκBp65

We used RNA interference against NFκBp65 to substantiate our findings on the molecular level. The efficient delivery of siRNA against NFκBp65 inhibited spontaneous proliferation and led to increased expression of α-SMA in MSCs from preterm infants with moderate or severe BPD (Figure 7).

These data suggest that NFκBp65 is responsible for the regulation of proliferation and expression of α-SMA in MSCs. Next, we focused on identifying the cause of the accumulation of NFκBp65.

Alterations in MSCs characterized by pro-inflammatory cytokines

The pulmonary inflammatory response in preterm infants is characterized by an imbalance of pro-inflammatory cytokines and growth factors. IL-1β and TNF-α represent important contributors to the inflammatory response in the preterm lung (42, 43). Measurements of IL-1β in the supernatant of tracheal aspirates confirmed a positive association between higher levels of IL-1β and an increased PI (Figure 8A). Next, we mimicked the *in vivo* environment and stimulated MSCs with recombinant IL-1β and TNF-α. Both cytokines consistently increased the PI in a panel of cultured MSCs (Figure 8B−D). Furthermore, both cytokines induced the accumulation of NFκBp65 and reduced the expression of α-SMA (Figure 8B and C). The effect of cytokine stimulation was accompanied by the nuclear translocation of NFκBp65 (Figure 8E). Dose-response analyses revealed gradual transition to an inflammatory phenotype depending on the extent of the pro-inflammatory stimulus (Figure 8F). A one-time cytokine stimulation was sufficient to induce persistent alterations in the phenotype of MSCs (Figure 8G). These data agree with the previous observation indicating that phenotypic alterations in MSCs from preterm infants with severe BPD persisted for several passages under cell culture conditions.

Finally, RNA interference, used in the experimental setting shown in Figure 7, was modified so that the baseline level of nuclear NFκBp65 was not affected. Subsequent stimulation with IL-1β or TNF-α markedly reduced the nuclear accumulation of NFκBp65 and the PI after cytokine stimulation (Figure 9A−D).

Discussion

We identified a combination of phenotypic alterations in MSCs isolated from the tracheal aspirates of preterm infants; these MSCs allow for the prediction of better or worse pulmonary prognosis in these children. Surprisingly, we were able to clearly separate children with good and poor pulmonary prognosis in the relatively small patient cohort studied.

Molecular studies indicated a link between phosphorylation of IκBα, the nuclear accumulation of NFκBp65, and the development of severe BPD. The accumulation of NFκBp65, induced by IL-1β and TNF-α, was responsible for the increased proliferative capacity of MSCs and was accompanied by the reduced expression of α-SMA. Notably, a one-time *in vitro* stimulation led to persistent alterations in the MSC phenotype lasting for days. These alterations were identical to those observed in MSCs freshly isolated from preterm infants who later developed severe BPD. Taken together, our data clearly indicate that alteration in the MSC phenotype is a critical event in the development of BPD.

The data presented here support the dominant role of NFκB within the cellular pulmonary inflammatory response; NFκB represents a central transcription factor with respect to proliferation and inflammation in many inflammatory diseases (15, 18, 27). High expression levels of NFκB within the total cellular fraction of tracheal aspirates are associated with later development of BPD, but the detailed analyses of specific cellular fractions have not yet been conducted. Cellular fractions possess a heterogeneous composition; hence, the predictive value was limited in previous studies (2, 5). Because MSCs represent a very small cellular fraction (data not shown), the determination of the expression level of NFκBp65 in MSCs was not achievable in previous studies. Using cell sorting and single cell analyses to optimize

the procedure described here will enable early determination of proliferative capacity and expression of NFκB and α-SMA in the majority of patients as shown before (22, 48). Once this has been achieved, the determination of MSC phenotype may be a promising biomarker for predicting pulmonary outcome and establishing a protocol for early treatment decisions. The general applicability of this biomarker approach requires validation in an independent cohort of patients (13).

Inflammation, infection, exposure to mechanical ventilation, and oxygen toxicity are important risk factors in the pathogenesis of BPD. These factors induce excessive and prolonged secretion of pro-inflammatory cytokines. Therefore, dysregulation of cytokine and growth factor signaling is attributed to the development of BPD (13, 43). Under physiological conditions, resident pulmonary mesenchymal cells undergo a highly orchestrated process of myofibroblastic differentiation during lung development (24, 28, 40). Previous studies demonstrated substantial alterations in the pathways controlling the differentiation of MSCs into myofibroblasts; these pathways include PDGF receptor α, β catenin, and TGF-β1 signaling in BPD (33, 37, 38, 40). Here we provide molecular evidence that exposure to pro-inflammatory cytokines leads to a persistent aberrant phenotype, with reduced expression of α-SMA, in pulmonary MSCs. This study was not designed to determine the precise origin of these cells from the proximal or distal airways of the immature lung; however, these cells are of pulmonary origin and display a lung-specific phenotype (3). It is possible that the distortion of myofibroblastic differentiation by pulmonary inflammatory response contributes to the distortion of septation and interstitial fibrosis (16, 29, 37, 38, 40). Our results provide a better understanding of how accumulation of NFκBp65 misdirects the functions of MSCs.

Conversely, NFκB signaling is a key pathway and regulator in the regulation of development, growth, and resolution of inflammation (15, 18, 25, 41). Members of the

TNF family are an important class of activators of NFκB. The downstream effect of TNF family members depends on specific intracellular signal transduction and includes pro-survival functions (1, 10-12, 46). In accordance with this, animal studies have clearly demonstrated that a balanced activation status is critical for normal lung development, and that either overstimulation or inhibition of NFκB signaling leads to distortion in normal lung development and a BPD-like phenotype (19, 27). A recent study demonstrated a connection between NFκB signal transduction and the TGF-β pathway, which is another important signaling pathway involved in lung development (11). Not surprisingly, any distortion in the balance of these signaling pathways can lead to augmented lung injury, and can result in increased induction of apoptosis in mesenchymal progenitor cells (11). Therefore, the direct targeting of NFκB can further distort lung development (19). However, selective targeting of NFκB signaling in MSCs, or identifying decisive downstream signaling pathway(s) that lead to detrimental activity of NFκB, can yield new therapeutic options.

MSCs are readily obtainable from tracheal aspirates of ventilated preterm infants. Studies on these cells can yield further valuable insights into the pathogenesis of BPD (3, 16, 33). Thorough evaluation of the physiological functions of these MSCs and their distortion in the injured lung is prerequisite for developing efficient therapeutic interventions. Our results indicate that distorted proliferation, nuclear accumulation of NFκBp65, and reduction in the α-SMA content of MSCs are early key events associated with the development of severe BPD. This study shows that future therapeutic approaches, aiming to prevent or reduce the burden of BPD, should include studies on phenotypic alterations in pulmonary MSCs. The following two scenarios should be considered: 1.) Reversal of the inflammatory MSC phenotype as achieved using RNA interference in this study. 2.) Prophylactic

prevention of phenotypic alterations in MSCs. In addition to the emerging beneficial role of allograft MSCs (35), the crucial role of resident lung MSCs has been discussed with respect to numerous pulmonary disease states of childhood and adolescence. (6, 22, 23, 30, 45) Our results encourage future studies to further focus on resident pulmonary MSCs and their role in inflammation and subsequent development of BPD, and to further examine alterations in the MSC phenotype, which account for disease severity.

Acknowledgements

We gratefully acknowledge the preservation of tracheal aspirates from routine suctioning by the staff of the Neonatal Intensive Care Units at the Perinatal Center Munich Großhadern and Perinatal Center Gießen. We thank all the parents of the infants for their consent to participate in the study.

This work is part of the MD theses of TR and SH.

Grants

This work was supported by Stiftung Projekt Omnibus, Wilhelm-Vaillant Stiftung (both to HE), Friedrich-Baur-Stiftung 0030/2008 (to HE and CH), and FöFoLe #49-2009 (to HE and AS).

Disclosures

All authors declare that they have no conflicts of interest.

References

1. **Baader E, Toloczko A, Fuchs U, Schmid I, Beltinger C, Ehrhardt H, Debatin KM, Jeremias I**. Tumor necrosis factor-related apoptosis-inducing ligand-mediated proliferation of tumor cells with receptor-proximal apoptosis defects. *Cancer Res* 65: 7888-7895, 2005.
2. **Bourbia A, Cruz MA, Rozycki HJ**. NF-κB in tracheal lavage fluid from intubated premature infants: association with inflammation, oxygen, and outcome. *Arch Dis Child Fetal Neonatal Ed* 91: F36-F39, 2006.
3. **Bozyk PD, Popova AP, Bentley JK, Goldsmith AM, Linn MJ, Weiss DJ, Hershenson MB**. Mesenchymal stromal cells from neonatal tracheal aspirates demonstrate a pattern of lung-specific gene expression. *Stem Cells Dev* 20: 1995-2007, 2011.
4. **Bry K, Whitsett JA, Lappalainen U**. IL-1β disrupts postnatal lung morphogenesis in the mouse. *Am J Respir Cell Mol Biol* 36: 32-42, 2007.
5. **Cheah F-C, Hampton MB, Darlow BA, Winterbourn CC, Vissers MC**. Detection of apoptosis by caspase-3 activation in tracheal aspirate neutrophils from premature infants: relationship with NF-κB activation. *J Leukoc Biol* 77: 432-437, 2005.
6. **Chow K, Fessel JP, Kaoriihida S, Schmidt EP, Gaskill C, Alvarez D, Graham B, Harrison DG, Wagner DH, Jr., Nozik-Grayck E, West JD, Klemm DJ, Majka SM**. Dysfunctional resident lung mesenchymal stem cells contribute to pulmonary microvascular remodeling. *Pulm Circ* 3: 31-49, 2013.
7. **Coalson JJ**. Pathology of bronchopulmonary dysplasia. *Semin Perinatol* 30: 179-184, 2006.
8. **Collins JJ, Thebaud B**. Lung mesenchymal stromal cells in development and disease: to serve and protect? *Antioxid Redox Signal* 21: 1849-1862, 2014.
9. **Dominici M, Le Blanc K, Mueller I, Slaper-Cortenbach I, Marini F, Krause D, Deans R, Keating A, Prockop D, Horwitz E**. Minimal criteria for defining multipotent mesenchymal stromal cells. The International Society for Cellular Therapy position statement. *Cytotherapy* 8: 315-317, 2006.
10. **Ehrhardt H, Fulda S, Schmid I, Hiscott J, Debatin K-M, Jeremias I**. TRAIL induced survival and proliferation in cancer cells resistant towards TRAIL-induced apoptosis mediated by NF-[kappa] B. *Oncogene* 22: 3842, 2003.
11. **Ehrhardt H, Pritzke T, Oak P, Kossert M, Biebach L, Forster K, Koschlig M, Alvira CM, Hilgendorff A**. Absence of TNF-alpha enhances inflammatory response in the newborn lung undergoing mechanical ventilation. *Am J Physiol Lung Cell Mol Physiol* 310: L909-918, 2016.
12. **Ehrhardt H, Wachter F, Grunert M, Jeremias I**. Cell cycle-arrested tumor cells exhibit increased sensitivity towards TRAIL-induced apoptosis. *Cell Death Dis* 4: e661, 2013.
13. **Förster K, Sass S, Ehrhardt H, Mous DS, Rottier RJ, Oak P, Schulze A, Flemmer AW, Gronbach J, Hübener C**. Early Identification of Bronchopulmonary Dysplasia Using Novel Biomarkers by Proteomic Screening. *Am J Respir Crit Care Med* 2017.
14. **Gough A, Linden M, Spence D, Patterson CC, Halliday HL, McGarvey LP**. Impaired lung function and health status in adult survivors of bronchopulmonary dysplasia. *Eur Respir J* 43: 808-816, 2014.
15. **Hayden MS, Ghosh S**. NF-κB, the first quarter-century: remarkable progress and outstanding questions. *Genes Dev* 26: 203-234, 2012.
16. **Hennrick KT, Keeton AG, Nanua S, Kijek TG, Goldsmith AM, Sajjan US, Bentley JK, Lama VN, Moore BB, Schumacher RE**. Lung cells from neonates show a mesenchymal stem cell phenotype. *Am J Respir Crit Care Med* 175: 1158-1164, 2007.
17. **Hilgendorff A, Reiss I, Ehrhardt H, Eickelberg O, Alvira CM**. Chronic lung disease in the preterm infant. Lessons learned from animal models. *Am J Respir Cell Mol Biol* 50: 233-245, 2014.
18. **Imanifooladi AA, Yazdani S, Nourani MR**. The role of nuclear factor-κB in inflammatory lung disease. *Inflamm Allergy Drug Targets* 9: 197-205, 2010.
19. **Iosef C, Alastalo T-P, Hou Y, Chen C, Adams ES, Lyu S-C, Cornfield DN, Alvira CM**. Inhibiting NF-κB in the developing lung disrupts angiogenesis and alveolarization. *Am J Physiol Lung Cell Mol Physiol* 302: L1023-L1036, 2012.

20. **Islam JY, Keller RL, Aschner JL, Hartert TV, Moore PE**. Understanding the Short- and Long-Term Respiratory Outcomes of Prematurity and Bronchopulmonary Dysplasia. *Am J Respir Crit Care Med* 192: 134-156, 2015.
21. **Jobe AH, Bancalari E**. Bronchopulmonary dysplasia. *Am J Respir Crit Care Med* 163: 1723-1729, 2001.
22. **Jun D, Garat C, West J, Thorn N, Chow K, Cleaver T, Sullivan T, Torchia EC, Childs C, Shade T**. The Pathology of Bleomycin-Induced Fibrosis Is Associated with Loss of Resident Lung Mesenchymal Stem Cells That Regulate Effector T-cell Proliferation. *Stem Cells* 29: 725-735, 2011.
23. **Khan P, Gazdhar A, Savic S, Lardinois D, Roth M, Tamm M, Geiser T, Hostettler K**. 118 Lung-derived mesenchymal stem cells exert anti-fibrotic effects in vitro. *Chest* 151: A15, 2017.
24. **Kugler MC, Loomis CA, Zhao Z, Cushman JC, Liu L, Munger JS**. Sonic Hedgehog Signaling Regulates Myofibroblast Function during Alveolar Septum Formation in Murine Postnatal Lung. *Am J Respir Cell Mol Biol* 57: 280-293, 2017.
25. **Lawrence T, Fong C**. The resolution of inflammation: anti-inflammatory roles for NF-κB. *Int J Biochem Cell Biol* 42: 519-523, 2010.
26. **Lee B, Sharron M, Montaner LJ, Weissman D, Doms RW**. Quantification of CD4, CCR5, and CXCR4 levels on lymphocyte subsets, dendritic cells, and differentially conditioned monocyte-derived macrophages. *Proc Natl Acad Sci U S A* 96: 5215-5220, 1999.
27. **Londhe VA, Maisonet TM, Lopez B, Jeng J-M, Xiao J, Li C, Minoo P**. Conditional deletion of epithelial IKKβ impairs alveolar formation through apoptosis and decreased VEGF expression during early mouse lung morphogenesis. *Respir Res* 12: 134, 2011.
28. **McGowan SE**. Paracrine cellular and extracellular matrix interactions with mesenchymal progenitors during pulmonary alveolar septation. *Birth Defects Res A Clin Mol Teratol* 100: 227-239, 2014.
29. **Mobius MA, Rudiger M**. Mesenchymal stromal cells in the development and therapy of bronchopulmonary dysplasia. *Mol Cell Pediatr* 3: 18, 2016.
30. **Möbius MA, Thébaud B**. Bronchopulmonary Dysplasia–Where have all the Stem Cells gone? Origin and (potential) function of resident lung stem cells. *Chest* 2017.
31. **Nestle F, Zheng X-G, Thompson C, Turka L, Nickoloff B**. Characterization of dermal dendritic cells obtained from normal human skin reveals phenotypic and functionally distinctive subsets. *J Immunol* 151: 6535-6545, 1993.
32. **Nicoletti I, Migliorati G, Pagliacci MC, Grignani F, Riccardi C**. A rapid and simple method for measuring thymocyte apoptosis by propidium iodide staining and flow cytometry. *J Immunol Methods* 139: 271-279, 1991.
33. **Oak P, Pritzke T, Thiel I, Koschlig M, Mous DS, Windhorst A, Jain N, Eickelberg O, Foerster K, Schulze A, Goepel W, Reicherzer T, Ehrhardt H, Rottier RJ, Ahnert P, Gortner L, Desai TJ, Hilgendorff A**. Attenuated PDGF signaling drives alveolar and microvascular defects in neonatal chronic lung disease. *EMBO Mol Med* 9: 1504-1520, 2017.
34. **Pilling D, Fan T, Huang D, Kaul B, Gomer RH**. Identification of markers that distinguish monocyte-derived fibrocytes from monocytes, macrophages, and fibroblasts. *PLoS One* 4: e7475, 2009.
35. **Pittenger MF, Le Blanc K, Phinney DG, Chan JK**. MSCs: Scientific Support for Multiple Therapies. *Stem Cells Int* 2015: 280572, 2015.
36. **Pittenger MF, Mackay AM, Beck SC, Jaiswal RK, Douglas R, Mosca JD, Moorman MA, Simonetti DW, Craig S, Marshak DR**. Multilineage potential of adult human mesenchymal stem cells. *Science* 284: 143-147, 1999.
37. **Popova AP, Bentley JK, Anyanwu AC, Richardson MN, Linn MJ, Lei J, Wong EJ, Goldsmith AM, Pryhuber GS, Hershenson MB**. Glycogen synthase kinase-3beta/beta-catenin signaling regulates neonatal lung mesenchymal stromal cell myofibroblastic differentiation. *Am J Physiol Lung Cell Mol Physiol* 303: L439-448, 2012.
38. **Popova AP, Bentley JK, Cui TX, Richardson MN, Linn MJ, Lei J, Chen Q, Goldsmith AM, Pryhuber GS, Hershenson MB**. Reduced platelet-derived growth factor receptor expression is a

primary feature of human bronchopulmonary dysplasia. *Am J Physiol Lung Cell Mol Physiol* 307: L231-L239, 2014.

39. **Popova AP, Bozyk PD, Bentley JK, Linn MJ, Goldsmith AM, Schumacher RE, Weiner GM, Filbrun AG, Hershenson MB**. Isolation of tracheal aspirate mesenchymal stromal cells predicts bronchopulmonary dysplasia. *Pediatrics* 126: e1127-1133, 2010.

40. **Popova AP, Bozyk PD, Goldsmith AM, Linn MJ, Lei J, Bentley JK, Hershenson MB**. Autocrine production of TGF-β1 promotes myofibroblastic differentiation of neonatal lung mesenchymal stem cells. *Am J Physiol Lung Cell Mol Physiol* 298: L735-L743, 2010.

41. **Rahman A, Fazal F**. Blocking NF-κB: an inflammatory issue. *Proc Am Thorac Soc* 8: 497-503, 2011.

42. **Ryan RM, Ahmed Q, Lakshminrusimha S**. Inflammatory mediators in the immunobiology of bronchopulmonary dysplasia. *Clin Rev Allergy Immunol* 34: 174-190, 2008.

43. **Shahzad T, Radajewski S, Chao C-M, Bellusci S, Ehrhardt H**. Pathogenesis of bronchopulmonary dysplasia: when inflammation meets organ development. *Mol Cell Pediatr* 3: 23, 2016.

44. **Simmons DL, Walker C, Power C, Pigott R**. Molecular cloning of CD31, a putative intercellular adhesion molecule closely related to carcinoembryonic antigen. *J Exp Med* 171: 2147-2152, 1990.

45. **Sinclair K, Yerkovich ST, Chambers DC**. Mesenchymal stem cells and the lung. *Respirology* 18: 397-411, 2013.

46. **Wachter F, Grunert M, Blaj C, Weinstock DM, Jeremias I, Ehrhardt H**. Impact of the p53 status of tumor cells on extrinsic and intrinsic apoptosis signaling. *Cell Commun Signal* 11: 27, 2013.

Titles and legends to figures

Figure 1: Characterization of MSCs

Isolated cells displayed a homogenous and stable MSC phenotype. A: Description of the experimental procedure: MSCs were detected 1−4 days after cultivation of tracheal aspirates. MSCs were allowed to grow to confluence within 10−16 days before passaging. Experimental procedures were performed between passages 2 and 6. B: Using flow cytometry, cells expressed the surface receptors CD13, CD73, CD90, CD 105 which are typically expressed on MSCs, while they were not expressing markers of haematopoetic or myelopoetic cells (CD11b, CD14, CD34, CD45, and CXCR4). C: Cell differentiation into adipogenic (upper panel), osteogenic (center panel), and myofibroblastic (lower panel) cells was confirmed using Oil Red O staining, alizarin red staining, or immunofluorescence labeling for α-smooth muscle actin (α-SMA). D: Stability of cell characteristics was ensured until passage 6 for the proliferation index in n=20 different MSC cultures (upper panel) and for the content of α-SMA (lower panel). Statistical analysis was performed using an ANOVA and Bonferroni post-hoc adjusted pairwise comparison (NS=not significant).

Figure 2. Emergence and duration of the presence of MSCs in tracheal aspirates

The time point of first detection of MSCs and the duration of successful cultivation did not differ between groups defined by disease severity. Tracheal aspirates were cultured every other day during the entire period of invasive mechanical ventilation. MSC outgrowth is indicated by bars.

Figure 3: Determination of proliferative capacity of MSCs and induction of cell death

Cell proliferation was determined using Cellscreen automated computer-based light microscopy. Results were confirmed by complementary techniques. A: The proliferative capacity of MSCs was determined over time using Cellscreen. Red lines indicate the surface area covered by the cells, while blue lines indicate the uncovered surface area excluded from the red marked area. B: The proliferation index was introduced to standardize the well area covered at the start of experiments (right panel) as cell density varied between samples (left panel). Cellscreen analysis (C) and manual cell counts (D) yielded identical results in MSCs from different patients. E: The fraction of dead cells did not differ between samples. The mean from n=3 independent measurements is shown. Statistical analysis was performed using Student's *t*-test. *p<0.05, which indicates statistically significant differences. NS = not significant.

Figure 4. The proliferative capacity of MSCs as a predictor of the duration of mechanical ventilation and severity of BPD

The proliferation index was significantly increased in MSCs from preterms with severe BPD in the cohort from Table 1. (A) Statistical analysis was performed from three independent experiments performed between p2 and p6 using one-way ANOVA and post-hoc pairwise comparisons by means of t-tests with Bonferroni adjustment. *p<0.05 indicates statistically significant differences. B: The predictive value was verified using a proportional odds model. p=0.008 indicates statistically significant differences. C: The association between the PI and days of mechanical ventilatory support was demonstrated using linear regression. p=0.025 indicates statistically significant differences. The association remained statistically significant when the two outlying values were omitted from the analysis.

Figure 5. The proliferative capacity of MSCs is correlated with the nuclear accumulation of NFκBp65 and reduction in α-SMA expression

Nuclear accumulation of NFκBp65 was increased in MSCs with a higher PI. A: Nuclear NFκBp65 was increased in MSCs (left panel) that were selected for their high spontaneous proliferation (right panel). Lamin A served as loading control. The order of samples from the identical blot was rearranged (central and lower blot) and indicated by separating lines without any further manipulation. Student's *t*-test was used to test for differences between groups; $p<0.001$ indicates statistically significant differences. B: Computer-based image quantification was introduced to compare protein density between different gels as presented for nuclear NFκBp65. An internal standard deposited on each gel enabled comparison of different gels (standardized expression level). The relative NFκBp65 expression was calculated as NFκBp65 quantification / Lamin A quantification; standardized quantification was calculated by division by the internal standard. Different sections from identical gels (indicated by separated lines) are presented without any further manipulation. C: The expression level of NFκBp65 was significantly higher in preterms with severe BPD when the technique described in Figure 5B was applied to evaluate the total cohort. Nuclear extracts were available from n=42 patients. Statistical analysis was performed using one-way ANOVA and post-hoc pairwise comparisons by means of t-tests with Bonferroni adjustment. *$p<0.05$ indicates statistically significant differences. D: The predictive accuracy of NFκBp65 was verified using the proportional odds model. $p=0.015$ indicates statistically significant differences. E: Inhibition of IκBα phosphorylation by Iκκ2 inhibitor IV (10 μM) reduced proliferation in MSCs after 72 hours. Western blot analysis was performed after 48 hours. Statistical analysis was performed using a post-hoc Bonferroni adjusted pairwise comparison. The mean

from n=3 experiments is shown. *p<0.005 indicates statistically significant differences.

Figure 6. Protein expression levels in MSCs correlate with BPD severity and can serve as predictive markers for pulmonary outcome

Reduced expression of α-SMA together with an increased PI and augmented nuclear accumulation of NFκBp65 can serve to predict severe BPD. The expression level of other proteins showed no differences between MSC cultures. A: Using immunofluorescence, MSCs from 2 patients with mild or severe BPD did not differ in the expression levels of PDGF receptor α (PDGFRα), Collagen Iα, myosin heavy chain, while αα-SMA expression was reduced in MSCs obtained from the infant with severe BPD. B: In Western Blot, α-SMA expression was reduced in cytosolic extracts of selected MSCs from preterms with moderate or severe BPD. GAPDH served as loading control. The order of samples in the blot was rearranged without any further manipulation (indicated by separated lines). C: The expression level of α-SMA was significantly reduced in preterms with severe BPD in the total cohort when the technique from Figure 5B was applied to the total cohort. Cytosolic extracts were available from n=36 patients. Statistical analysis was performed using one-way ANOVA and post-hoc pairwise comparisons by means of *t*-tests with Bonferroni adjustment. *p<0.05 indicates statistical significance. D: The predictive accuracy of α-SMA was verified using the proportional odds model. p=0.018 indicates statistically significant differences. E: The receiver operating characteristic curve (ROC) for combining PI, NFκBp65, and α-SMA data from Figures 4A, 5C, and 6C in a logistic model predicted moderate/severe BPD with an area under the curve (AUC) of 0.847.

Figure 7. Using RNA interference to confirm the central role of NFκBp65 in alteration of the MSC phenotype

RNA interference against NFκBp65 reduced the proliferation of MSCs from n=15 randomly selected preterm infants with moderate or severe BPD. Cell growth was assessed by Cellscreen analysis for 72 hours starting twenty-four hours after transfection. Western blot analyses for NFκBp65 expression were performed 24 hours after transfection and for α-SMA after 72 hours. The calculated relative change in the proliferation index (%) is presented as the mean and 95% confidence interval compared with those of the untreated control group. Statistical significance was tested using a post-hoc Bonferroni adjusted pairwise comparison. *p=0.014 indicates statistically significant differences.

Figure 8. Increase in MSC proliferation and NFκBp65 accumulation mediated by pro-inflammatory cytokines IL-1β and TNF-α

Pro-inflammatory cytokines induced the identical changes observed in MSCs from preterm infants with unfavorable pulmonary outcome. A: IL-1β (ng/ml) standardized to sIgA (U/ml) determined in tracheal aspirate supernatants correlated to the proliferation index. Supernatants were available from n=29 infants. Statistical analysis was performed using linear regression. *p<0.05 indicates statistically significant differences. Stimulation of MSCs with IL-1β (B, 300 ng/ml) or TNF-α (C, 300 ng/ml) increased proliferation and nuclear NFκBp65 and reduced the content of cytosolic α-SMA. Different sections from the gel (indicated by separated lines) are presented without any further manipulation. Dots indicate the means of at least three different measurements ± SEM. D: Stimulation of n=12 randomly selected cell cultures with IL-1β and TNF-α increased spontaneous proliferation. Statistical

analysis was performed using a linear mixed model. * $p<0.05$ indicates a statistically significant difference versus control. E: Nuclear translocation of NFκBp65 was induced after stimulation with IL-1β (300 ng/ml) for the time periods indicated. F: Increasing the dosage of IL-1β from 3 to 300 ng/ml increased cell proliferation in MSCs. G: Separation of data from Figure 8F into 24-hour time intervals revealed a persistent increase in proliferation and reduction in α-SMA content. Statistical analysis was performed using Student's *t*-test (NS, not statistically significant).

Figure 9. Stimulation of MSCs with pro-proliferative cytokines induces a phenotype that is stable for at least 120 h

Modified RNA interference against NFκBp65 before stimulation with IL-1β (300 ng/ml; A and C) or TNF-α (300 ng/ml; B and D) reduced the nuclear accumulation of NFκBp65 and the PI. The order of western blot samples was rearranged as indicated by separated lines without any further manipulation. Statistical analysis was performed using ANOVA. *$p<0.05$ indicates statistically significant differences.

730 **Table 1. Patient characteristics of the study cohort**

	Complete study cohort	Preterm infants fulfilling inclusion criteria
Number of children	n=112	n=49
Gestational age (weeks)	26+0 (1+4)	25+6 (1+3)
Birth weight (g)	786 (241)	709 (279)
Male sex	70 (62.5%)	31 (63.3%)
Twin birth	46 (41.7%)	24 (48%)
Early onset infection	63 (56.3%)	31 (62%)
Antenatal steroids	103 (92%)	46 (92%)
Mechanical ventilatory support (days)	61 (28)	70 (22)
Any BPD	106 (94.6%)	49 (100%)
No BPD	6 (5.4%)	not included
Mild BPD	43 (38.4%)	19 (38%)
Moderate BPD	25 (22.3%)	16 (32%)
Severe BPD	24 (21.4%)	14 (28%)
Deceased	14 (12.5%)	not included

731 .

732 **Table 2. Detection of mesenchymal stromal cells in tracheal aspirates –**
733 **separation by BPD severity scores**

BPD grade	Mild	Moderate	Severe	p-value
Number of infants	19	13	17	p>0.05
Gestational age (weeks)	25+3 (7+3)	25+1 (0+6)	25+3 (1+5)	p>0.05
Birth weight (g)	704 (145)	707 (137)	709 (165)	p>0.05
Chorioamnionitis	9/19 (47.4%)	2/13 (15.4%)	4/14 (28.6%)	p>0.05
Day of first MSC isolation	9 (5)	8 (4)	8 (4)	p>0.05
Duration of presence of MSCs (days)	8 (7)	12 (8)	12 (7)	p>0.05
Maximum peak inspiratory pressure until culture establishment	14 (6)	13 (2)	16 (4)	p>0.05
Maximum FiO_2 (%) until culture establishment	29 (7)	33 (3)	40 (18)	p>0.05
Mechanical ventilatory support (days)	65 (13)	78 (13)	96 (33)	p<0.05
Proliferation index	2.04 (0.55)	2.7 (0.69)	2.87 (1.0)	p<0.05

734

735 **Table 3. Detection of MSCs in tracheal aspirates – separation by time**
736 **point of first appearance**

First appearance within	Day 0−7	Day 8−21	p-value
Number of infants	20	20	
Day of first MSC isolation	5 (2)	11 (4)	p<0.05
Gestational age (weeks)	24+6 (7+2)	26+0 (7+2)	p<0.05
Birth weight (g)	630 (98)	746 (143)	p<0.05
Mild BPD	7 (35%)	8 (40%)	p>0.05
Moderate BPD	5 (25%)	4 (20%)	p>0.05
Severe BPD	8 (40%)	8 (40%)	p>0.05
Maximum peak inspiratory pressure until culture establishment	14 (3)	16 (3)	p>0.05
Maximum FiO_2 (%) until culture establishment	34 (17)	34 (7)	p>0.05

Mechanical ventilatory support (days)	83 (33)	79 (15)	p>0.05
Proliferation index	2.6 (0.13)	2.24 (0.77)	p>0.05

737

Titles and legends for tables

Table 1

The relevant characteristics of the entire patient cohort of 112 preterm infants (<29 weeks of gestational age) and of the subgroup of patients fulfilling study inclusion criteria (see Materials and Methods for details) are presented. Children who died during intensive care therapy as a result of sepsis or severe intracranial bleeding before 36+0 weeks of gestational age were excluded (n=4). The mean values and standard deviations, or the percentage of children, are depicted. Higher order multiples were not present within the study cohort. Early onset infection was diagnosed if the infants showed two typical clinical signs of infection and a pathologic I/T ratio (≥ 0.2) and/or an increase in CRP ≥ 6 mg/l in the first 72 hours of life. A positive history of antenatal steroids included the application of a complete course of betamethasone or dexamethasone not longer than 7 days before birth. None of the children within the “no antenatal steroids group” were born beyond 12 hours of the initiation of the first course. The parameter “days of mechanical ventilatory support” includes any form of mechanical ventilation or continuous positive airway pressure (CPAP). The severity of BPD was classified according to the definition established by Jobe and Bancalari (21).

Table 2

Tracheal aspirates from 49 preterm infants were cultured at least every 2nd day during the period of mechanical ventilation and screened for the presence of MSCs. The mean values and standard deviations are presented. The number of patients with proven chorioamnionitis on pathological examination is presented in relation to the total number of patients. No pathological

examination could be performed on the placenta of three patients with severe BPD (two home births and one outborn child, where placenta was not sent for workup). Statistical analysis was performed using ANOVA on ranks and Chi-square to analyze for the presence of chorioamnionitis. PIP=peak inspiratory pressure, $Fi0_2$=fraction of oxygen in the breathing air.

Table 3

Preterm infants were separated by the time point of the first appearance of MSCs. Parameters were analyzed as in Table 1 and 2. Statistical analysis was performed using Student's *t*-test.

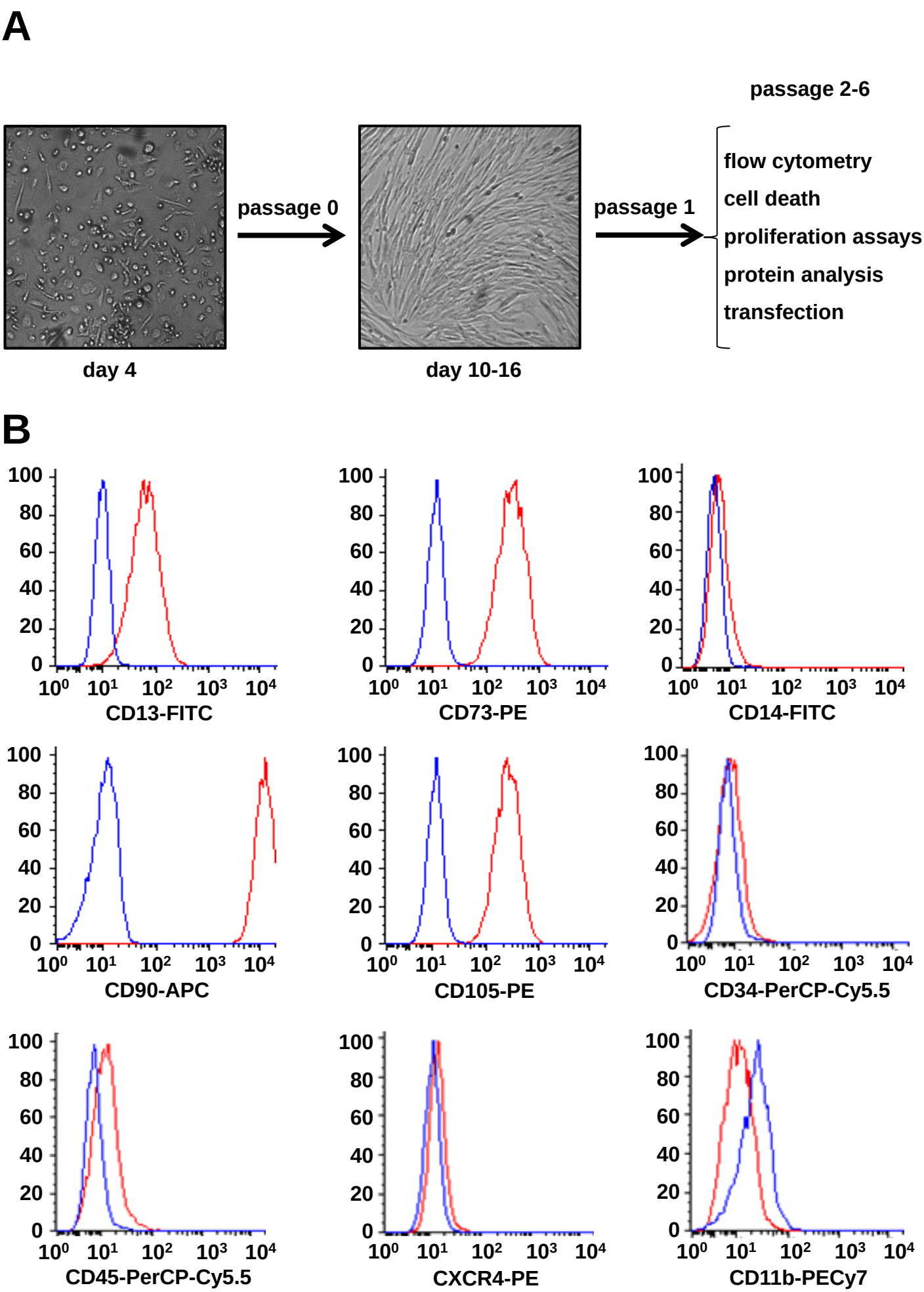

Figure 1

C

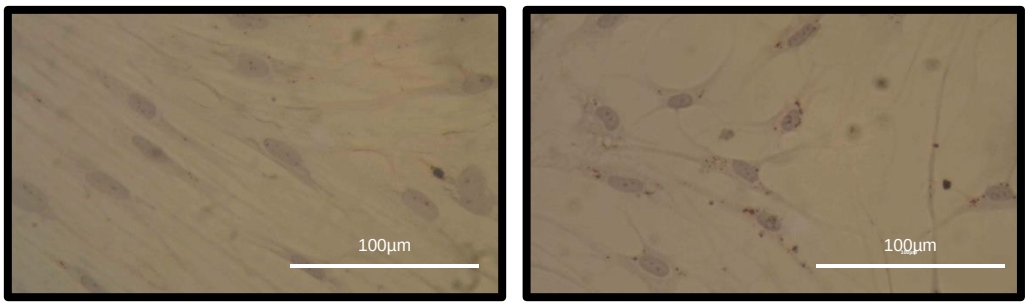

control | adipocyte differentiation

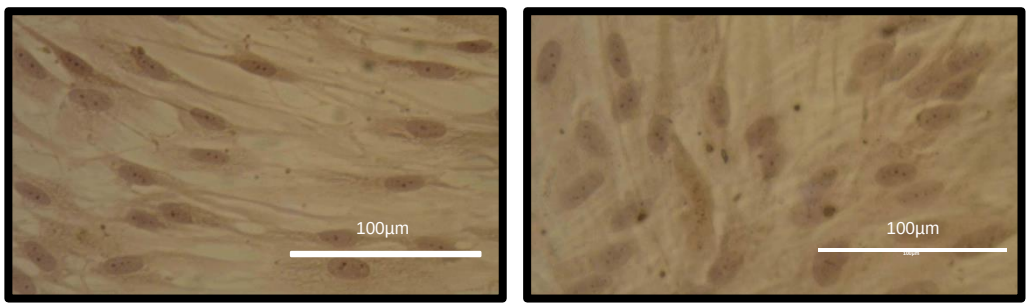

control | osteoblast differentiation

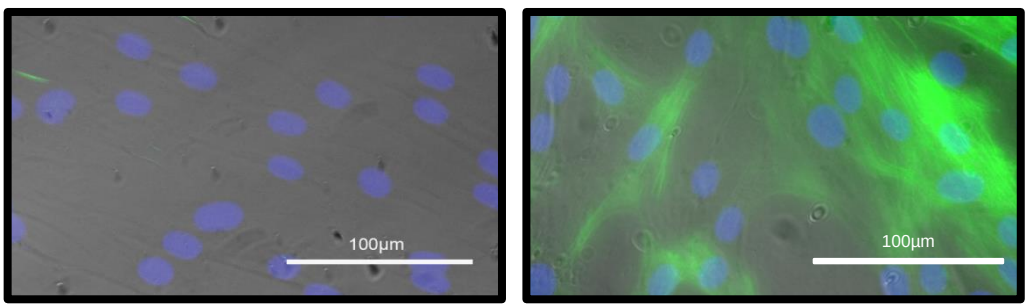

control | myofibroblast differentiation

Figure 1

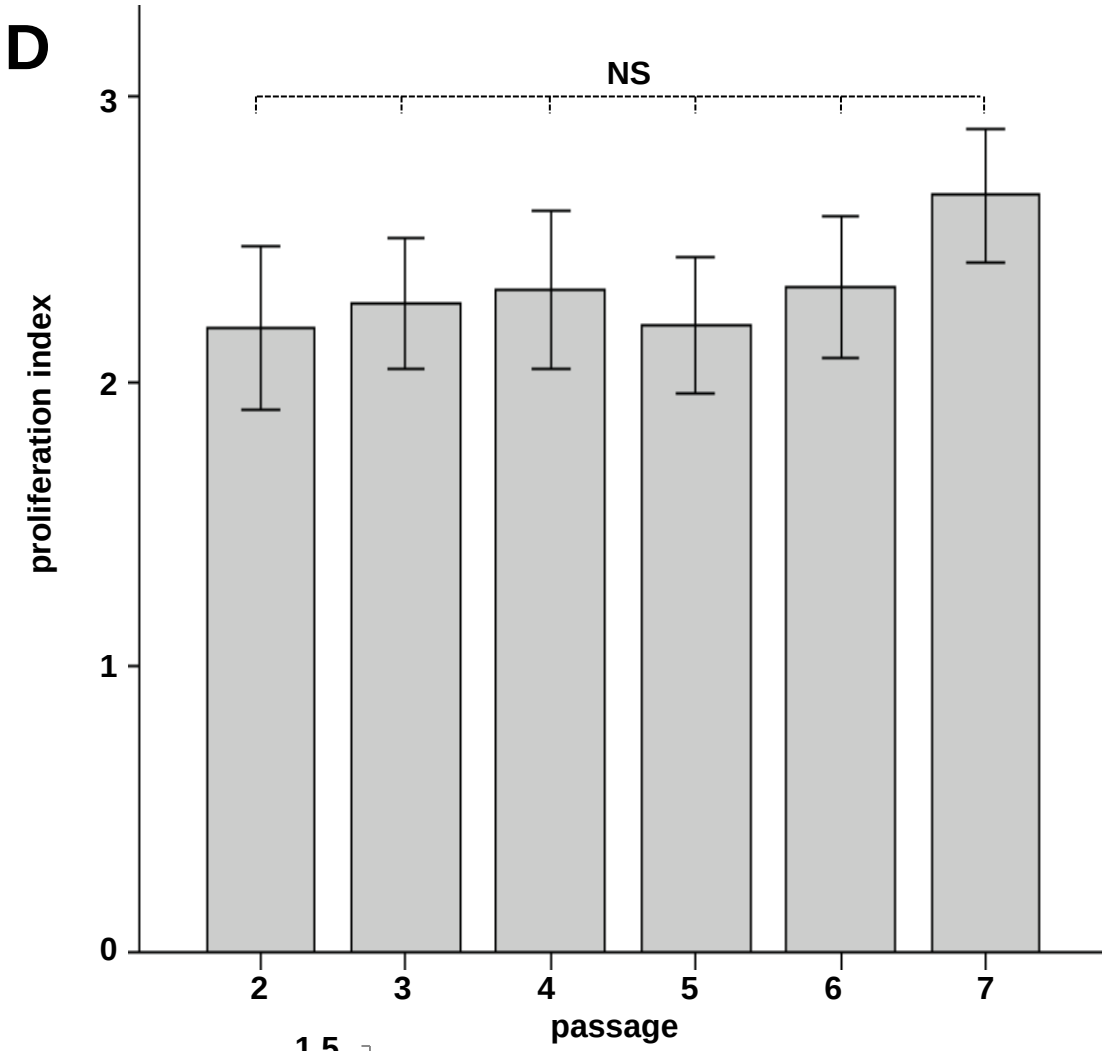

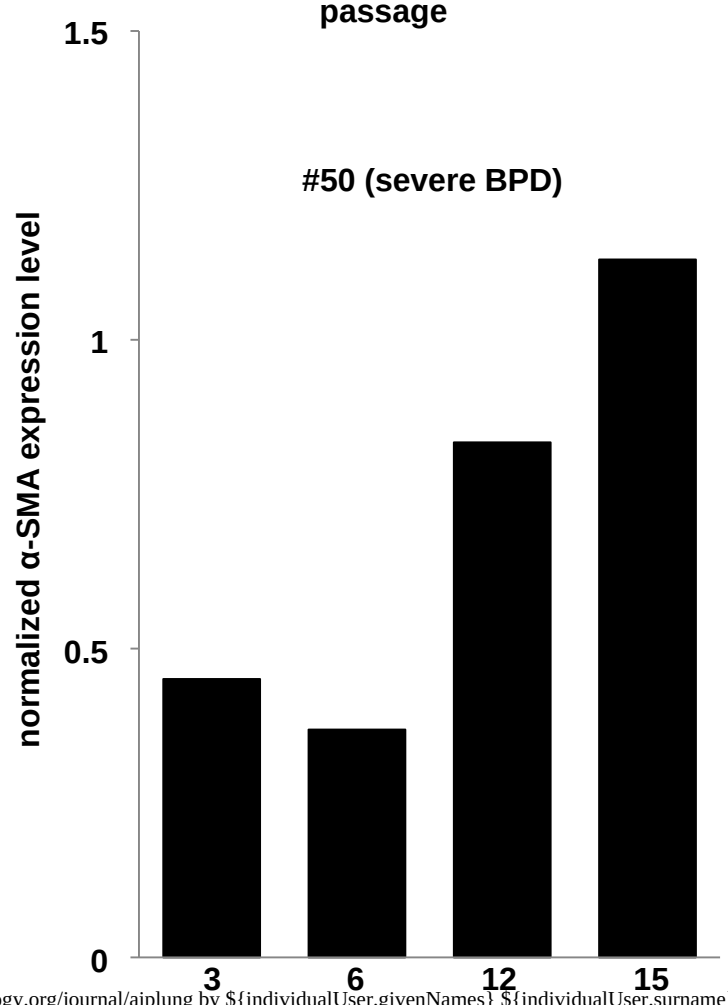

Figure 1

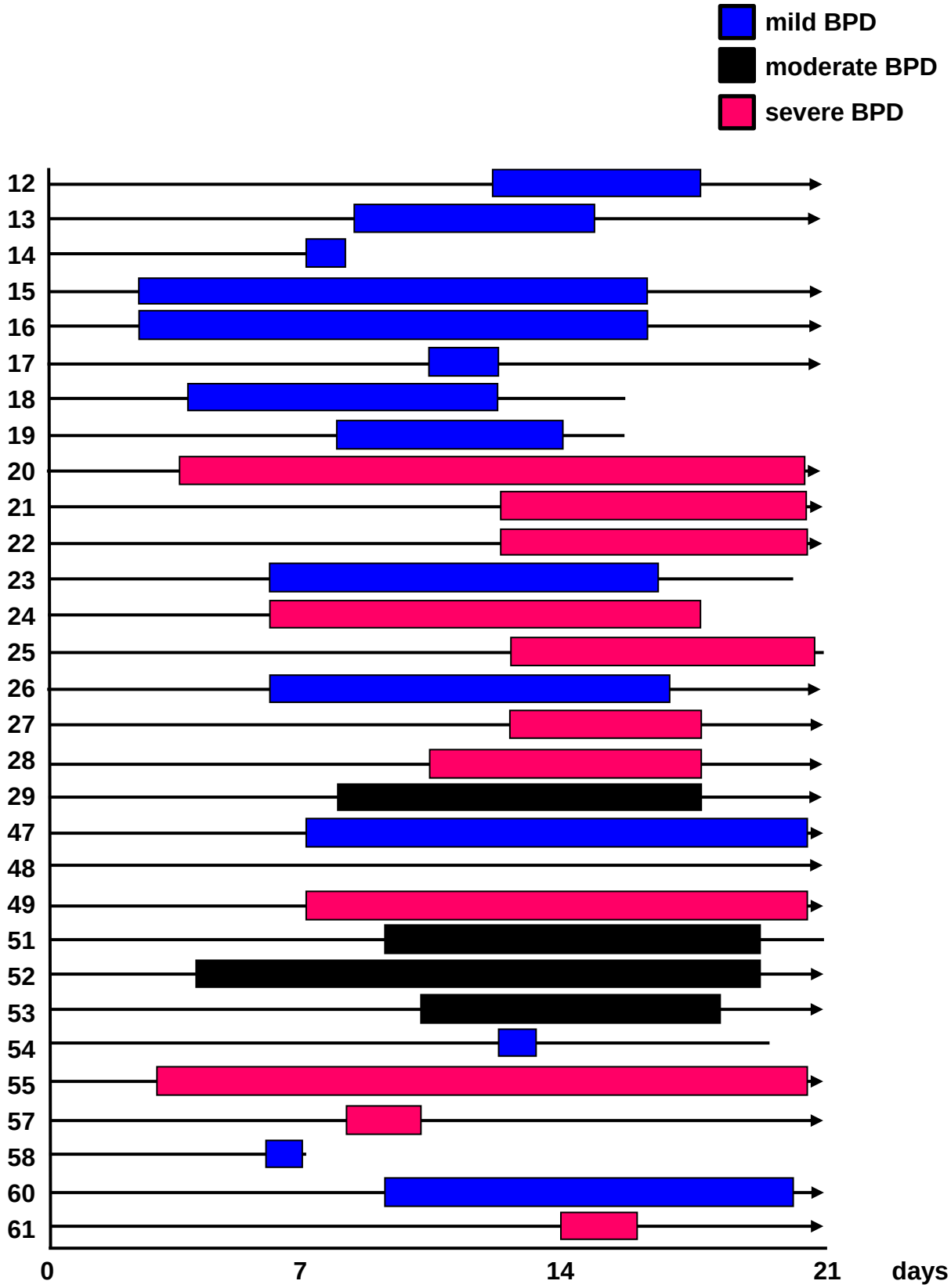

Figure 2

A

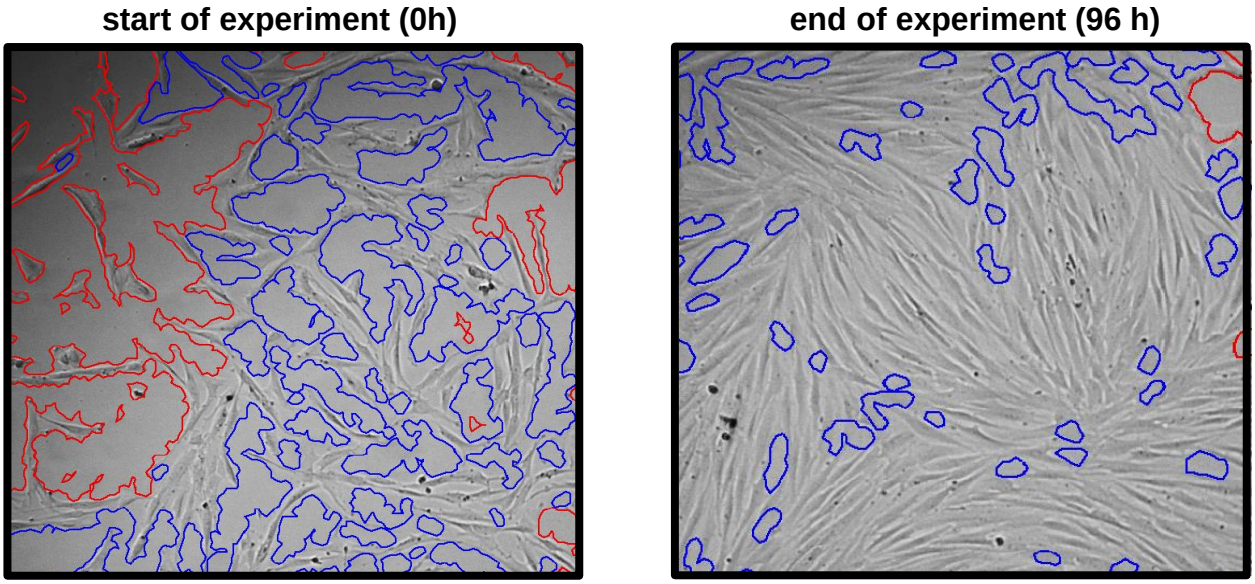

B

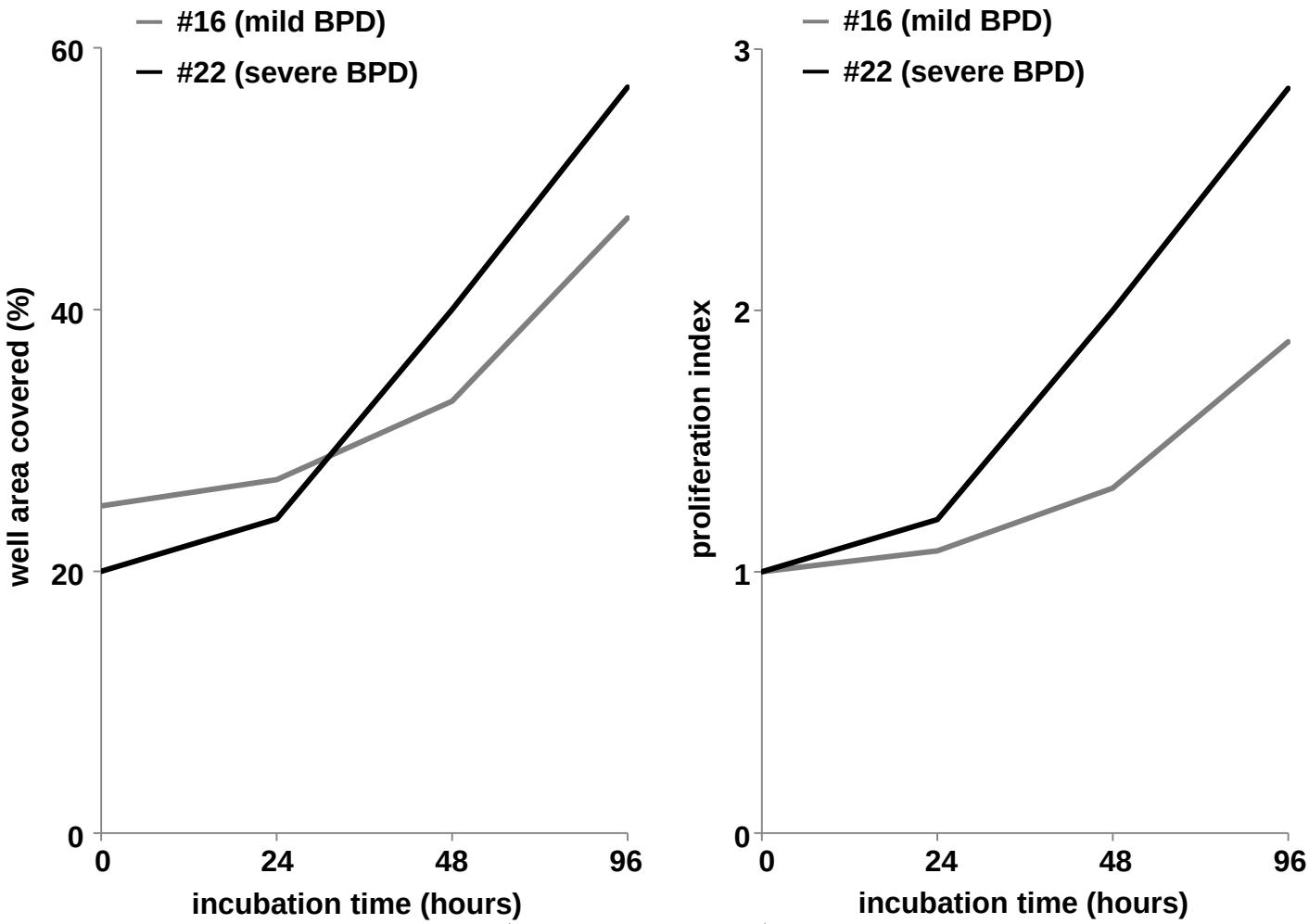

Figure 3

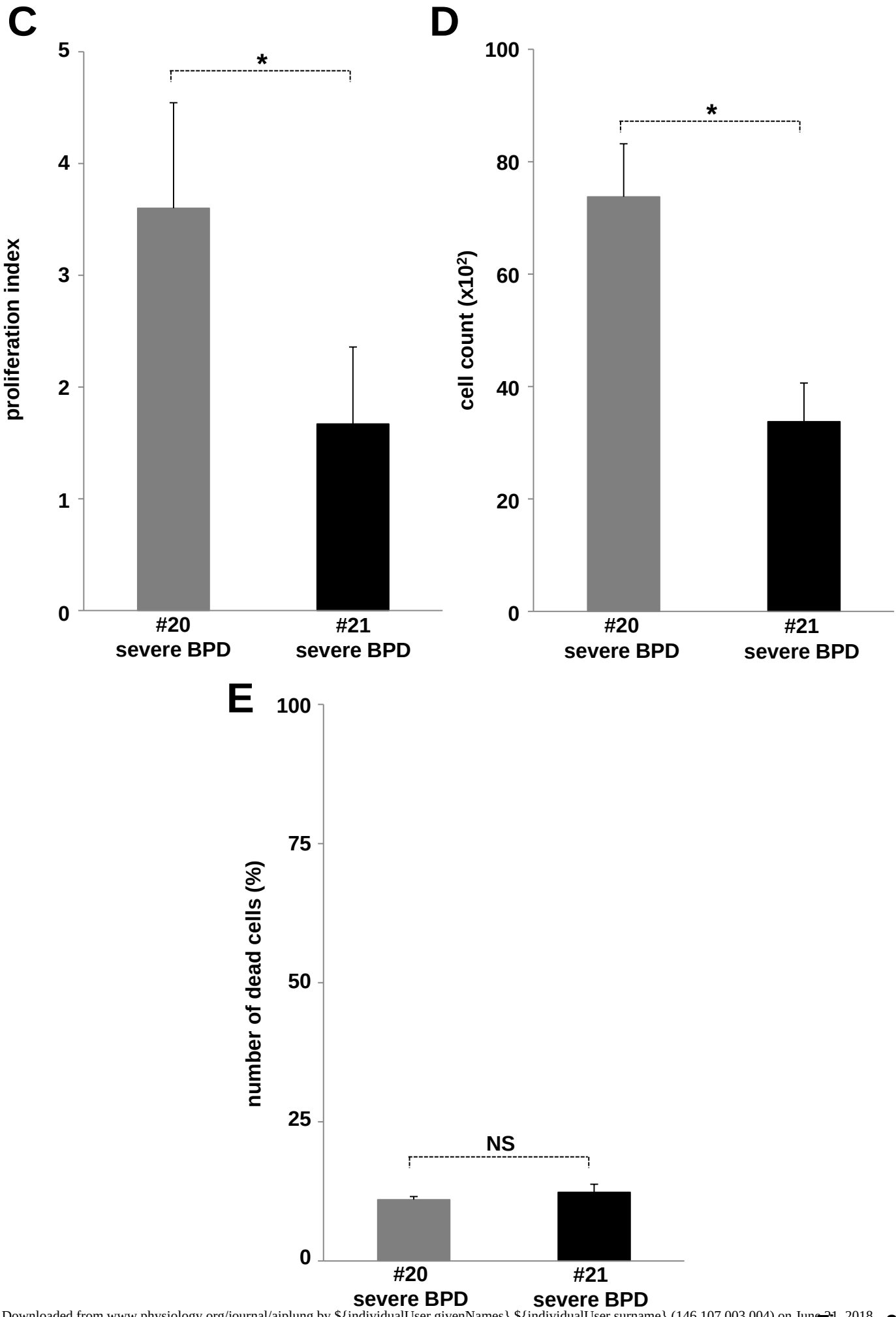

Figure 3

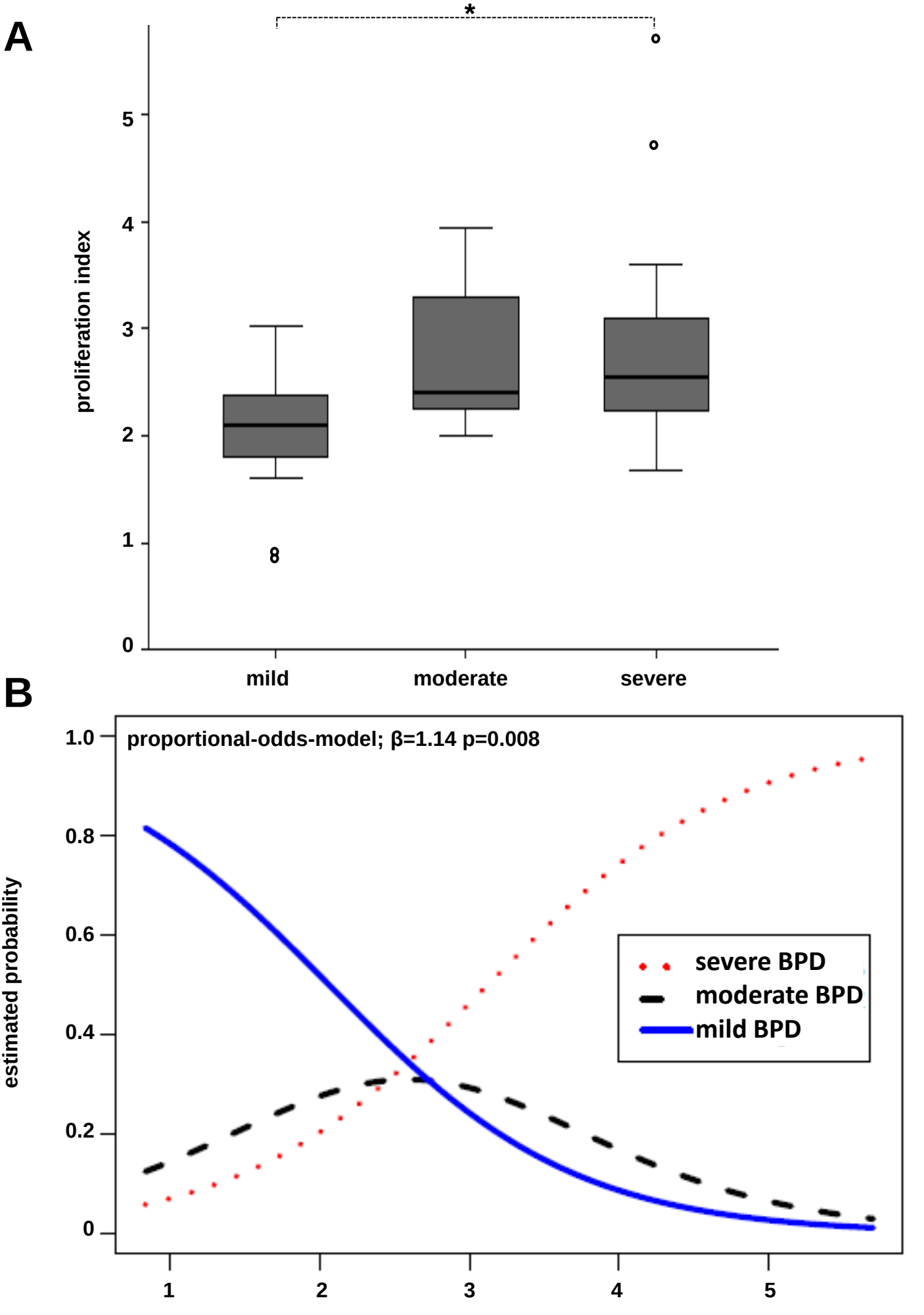

Figure 4

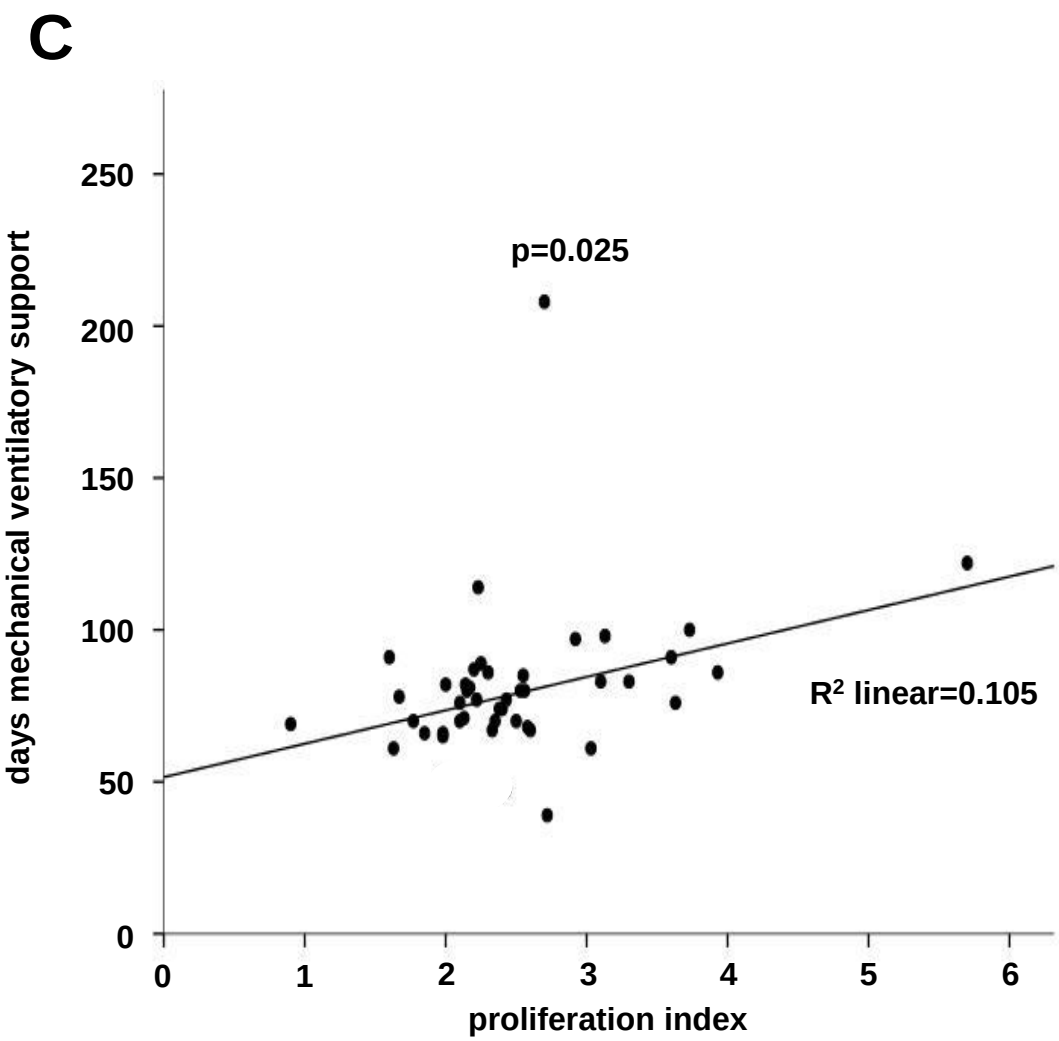

Figure 4

A

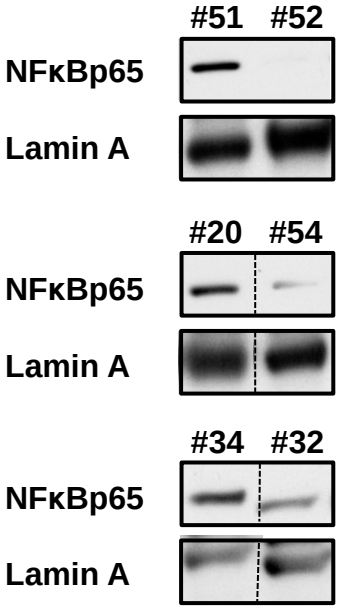

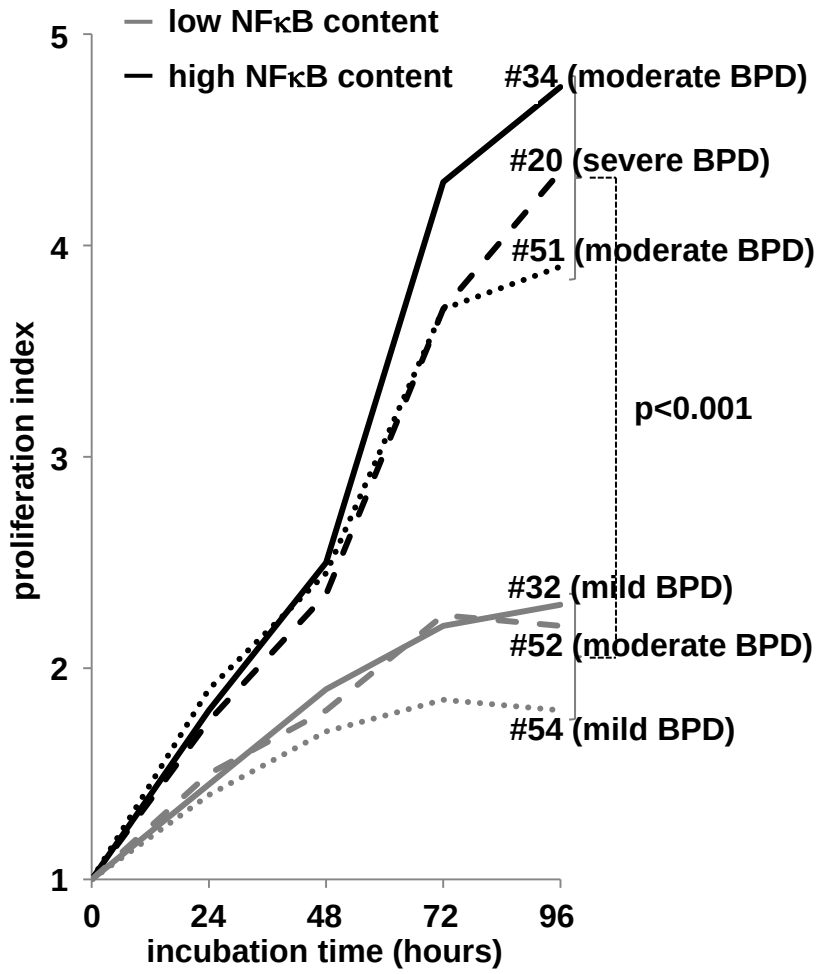

B

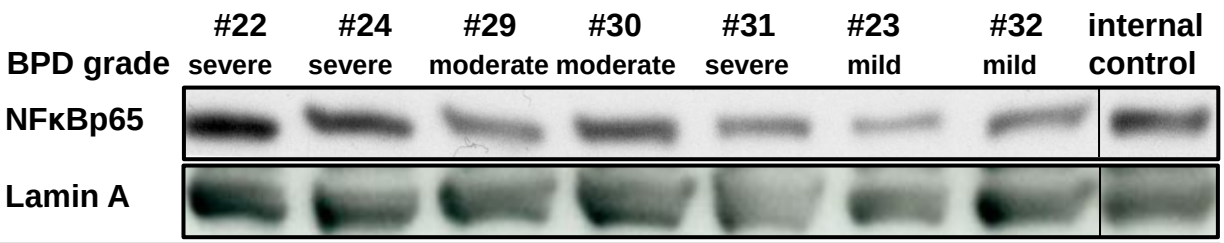

NFκBp65 quantification	95414	72241	45487	61247	31828	18547	39835	69247
Lamin A quantification	254695	237092	249505	269657	185287	177401	248743	218763
relative NFκBp65 expression	0.3746	0.3047	0.1823	0.2271	0.1718	0.1045	0.1601	0.3165
standardized NFκBp65 expression	1.1836	0.9627	0.5760	0.7175	0.5428	0.3302	0.5058	1.0000

Figure 5

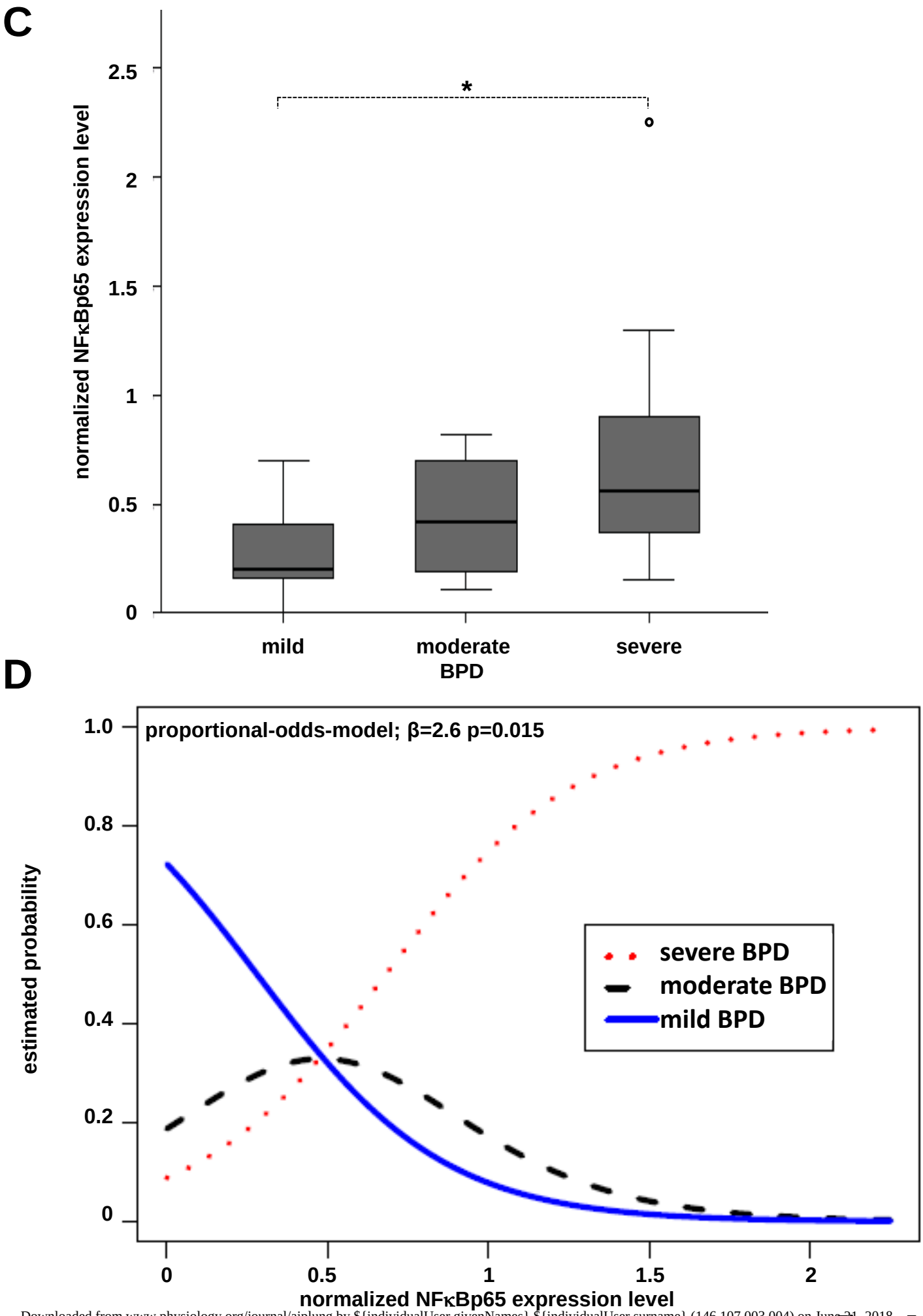

Figure 5

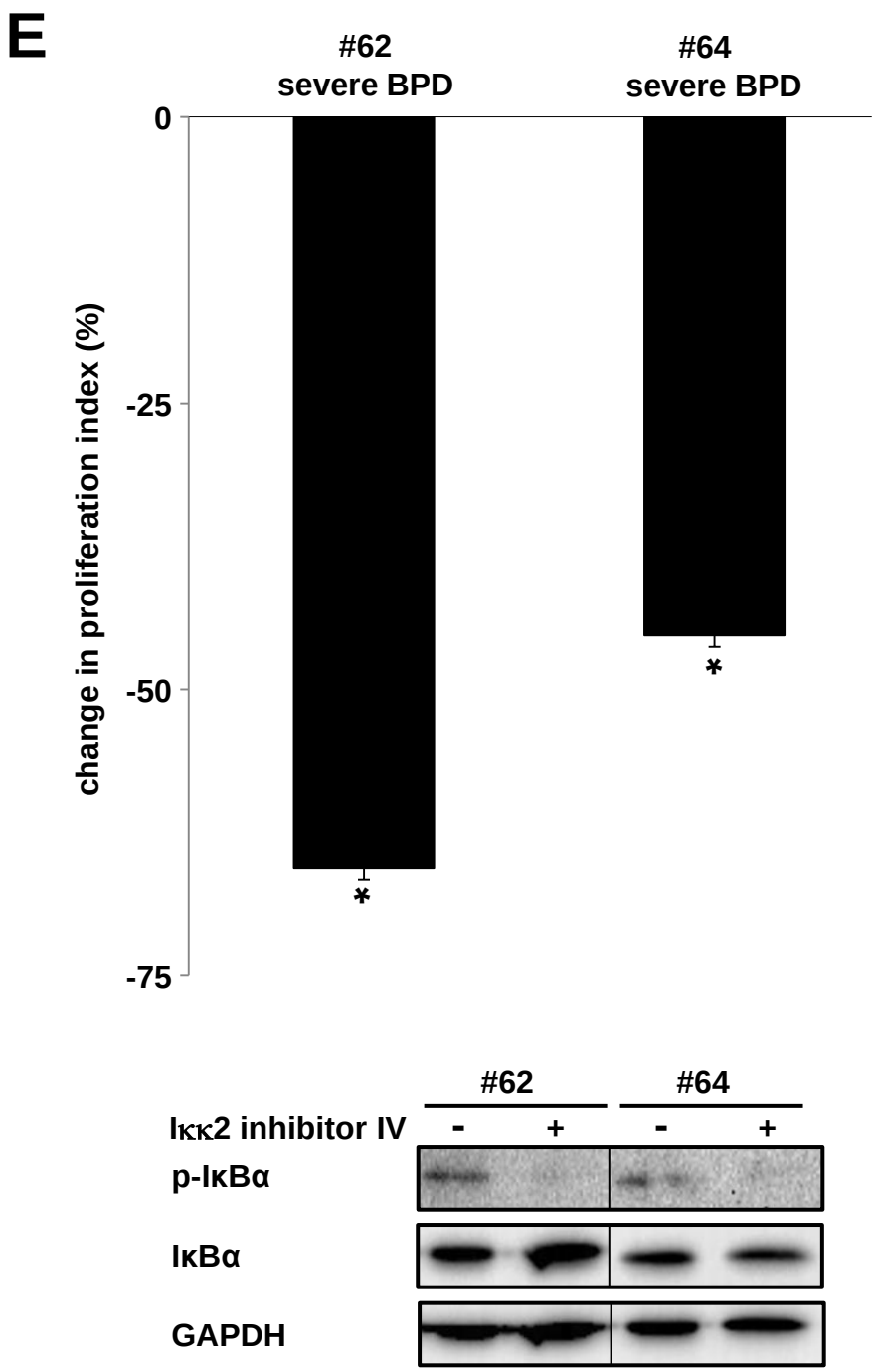

Figure 5

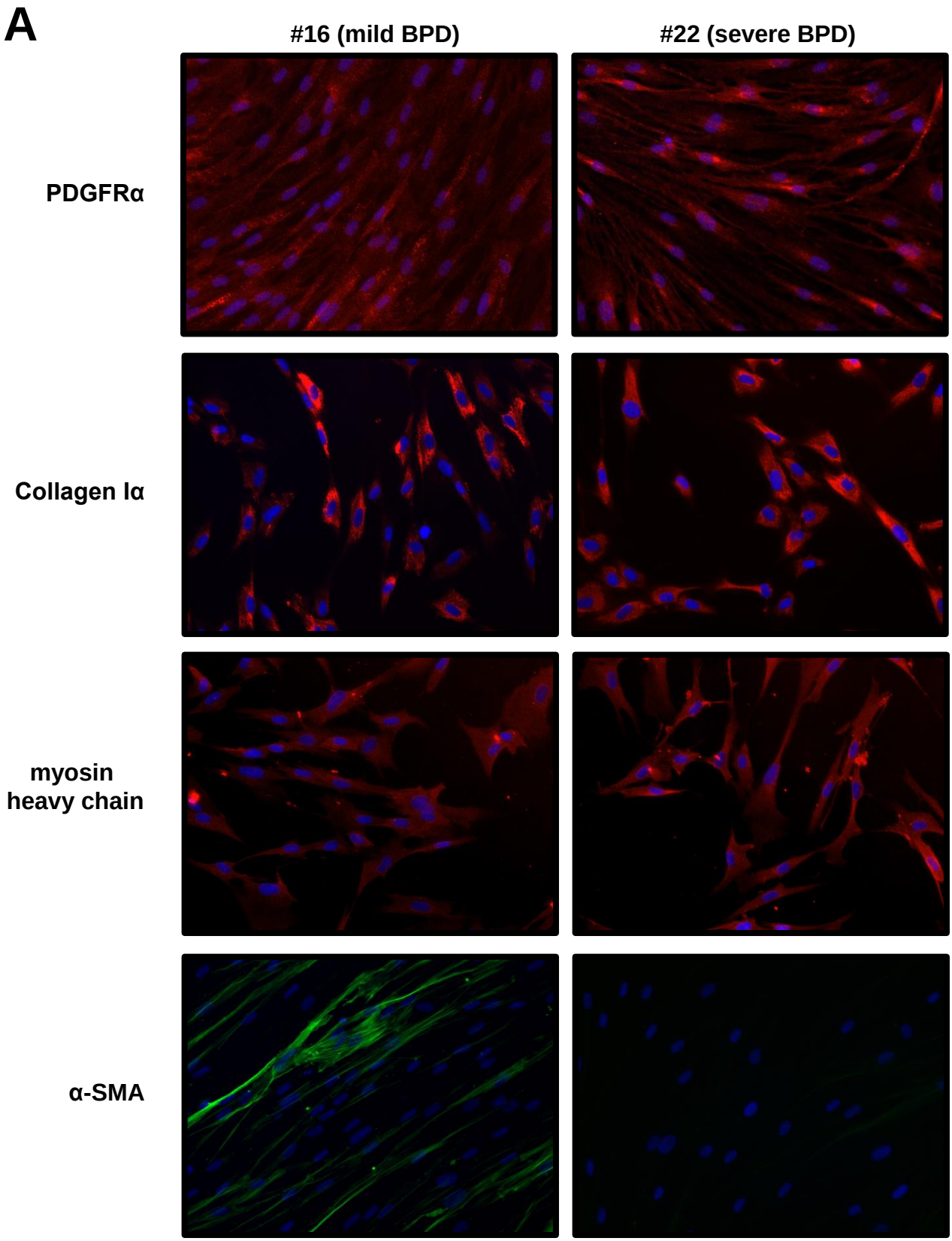

Figure 6

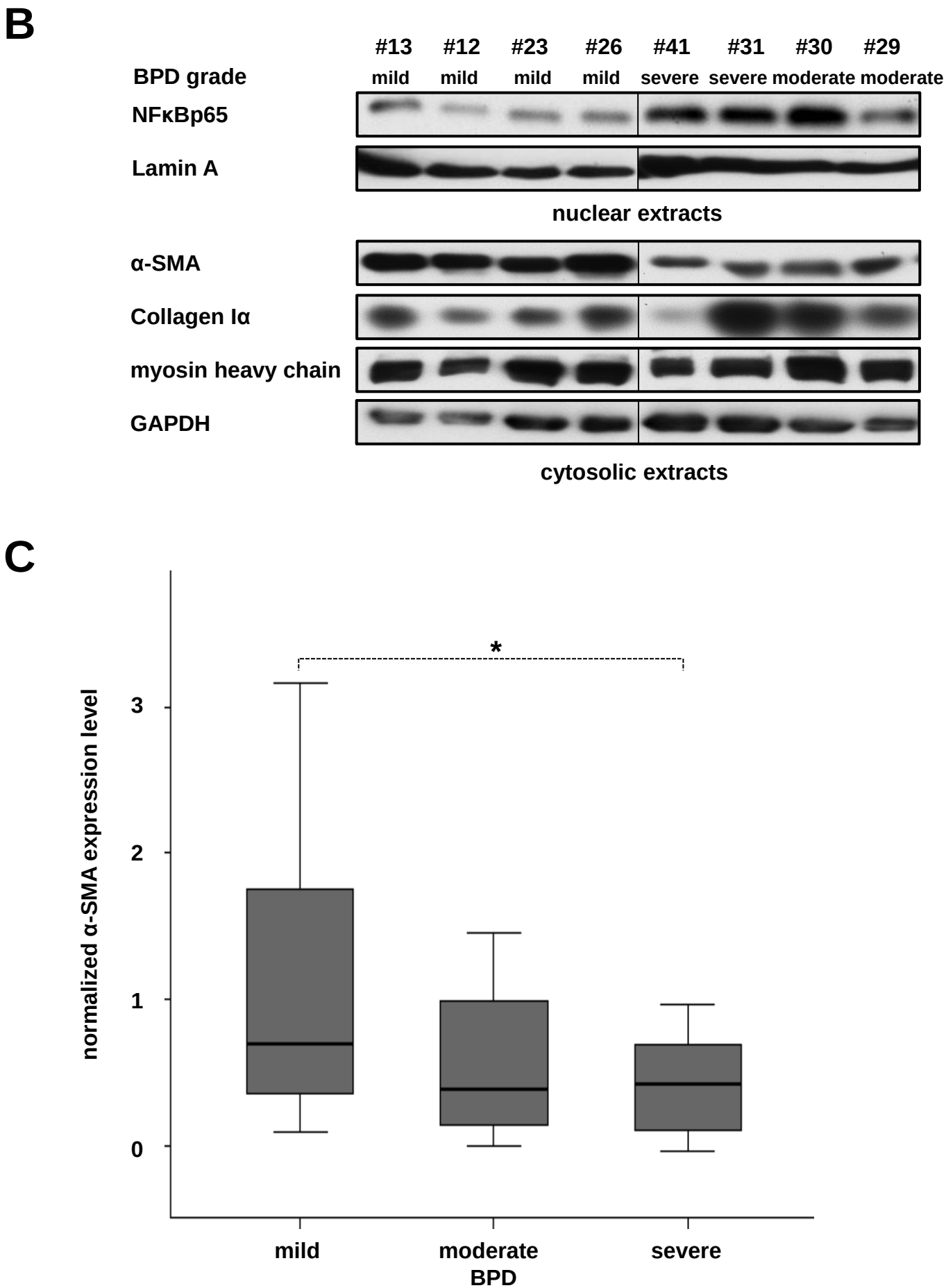

Figure 6

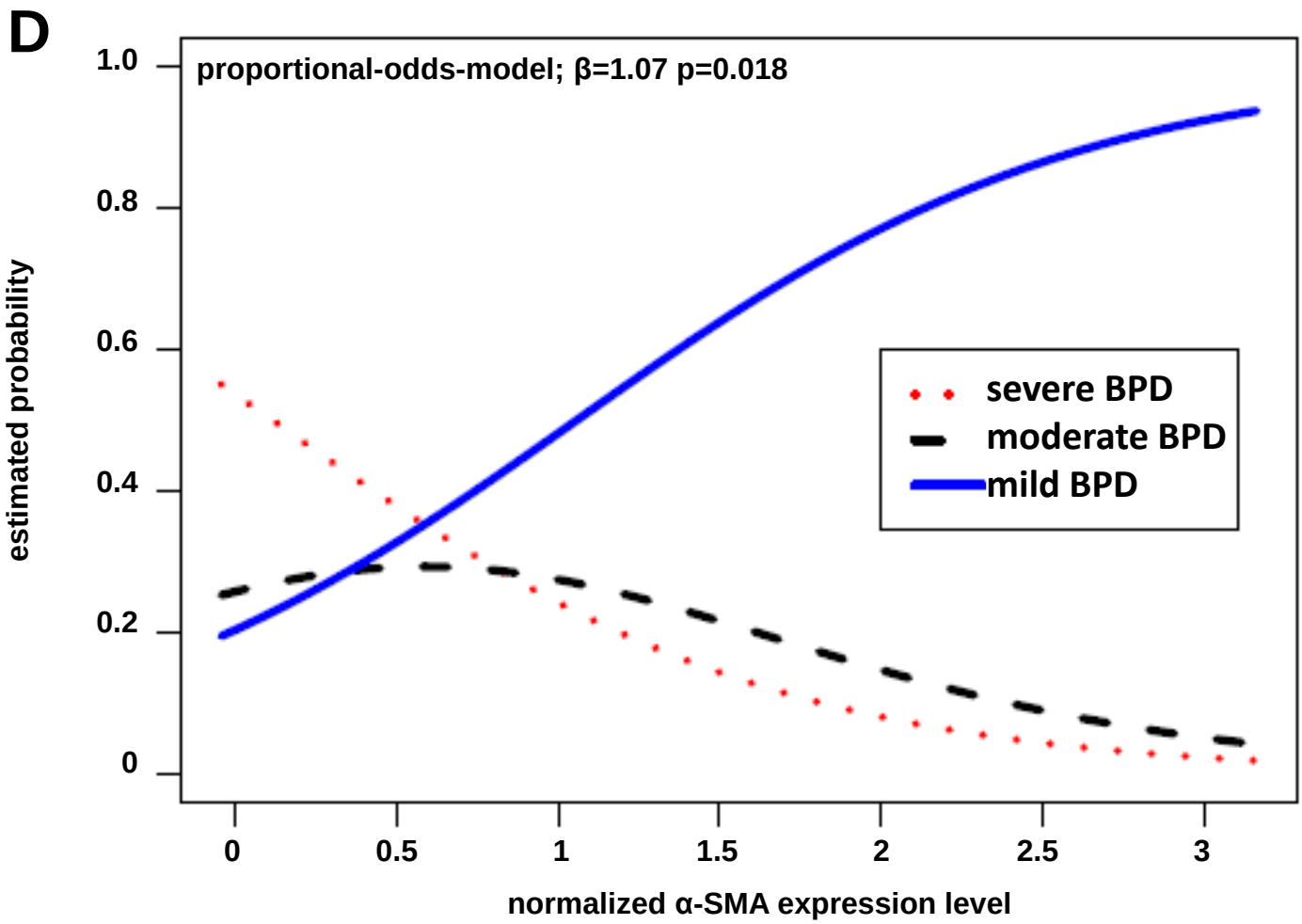

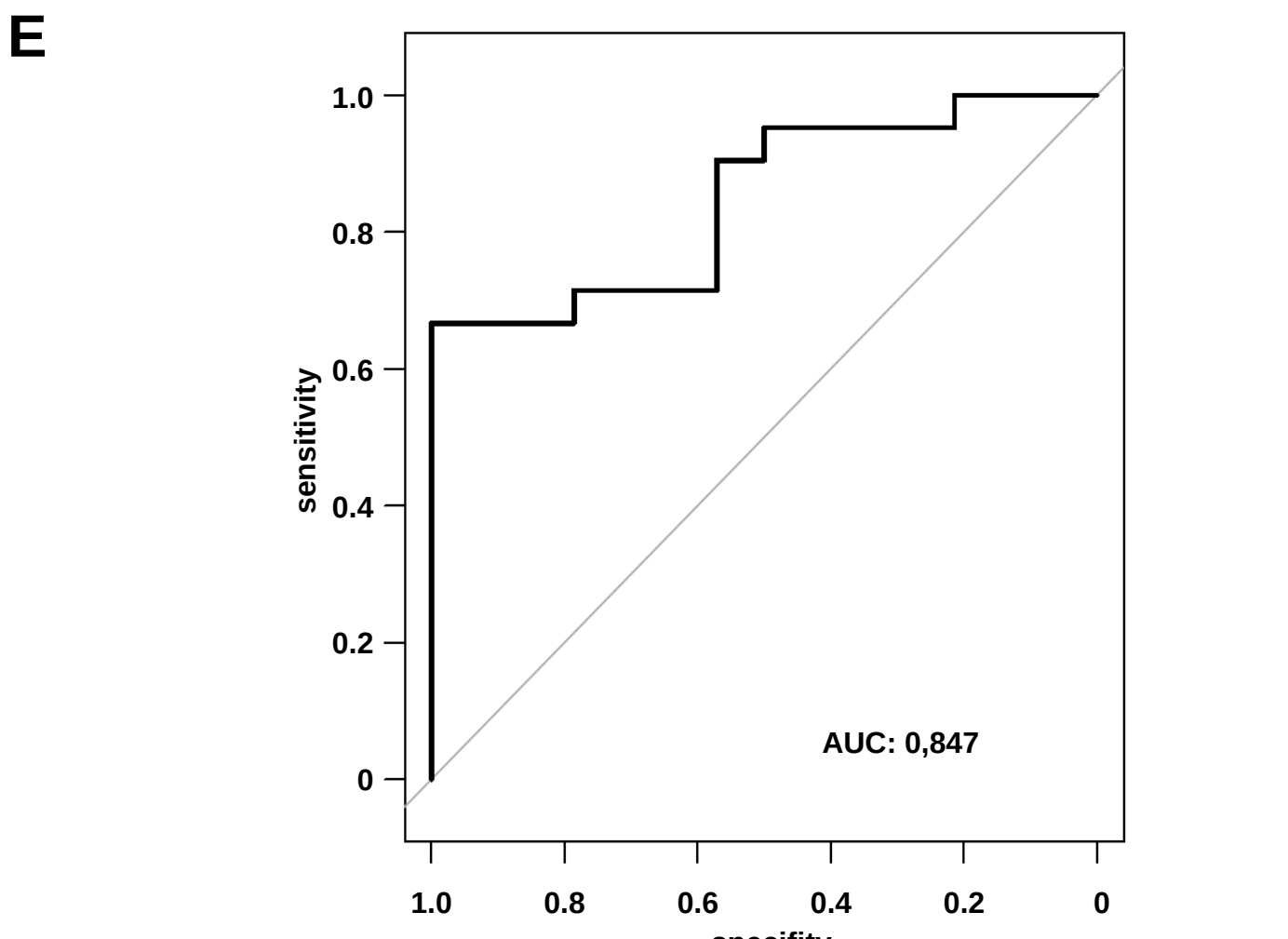

Figure 6

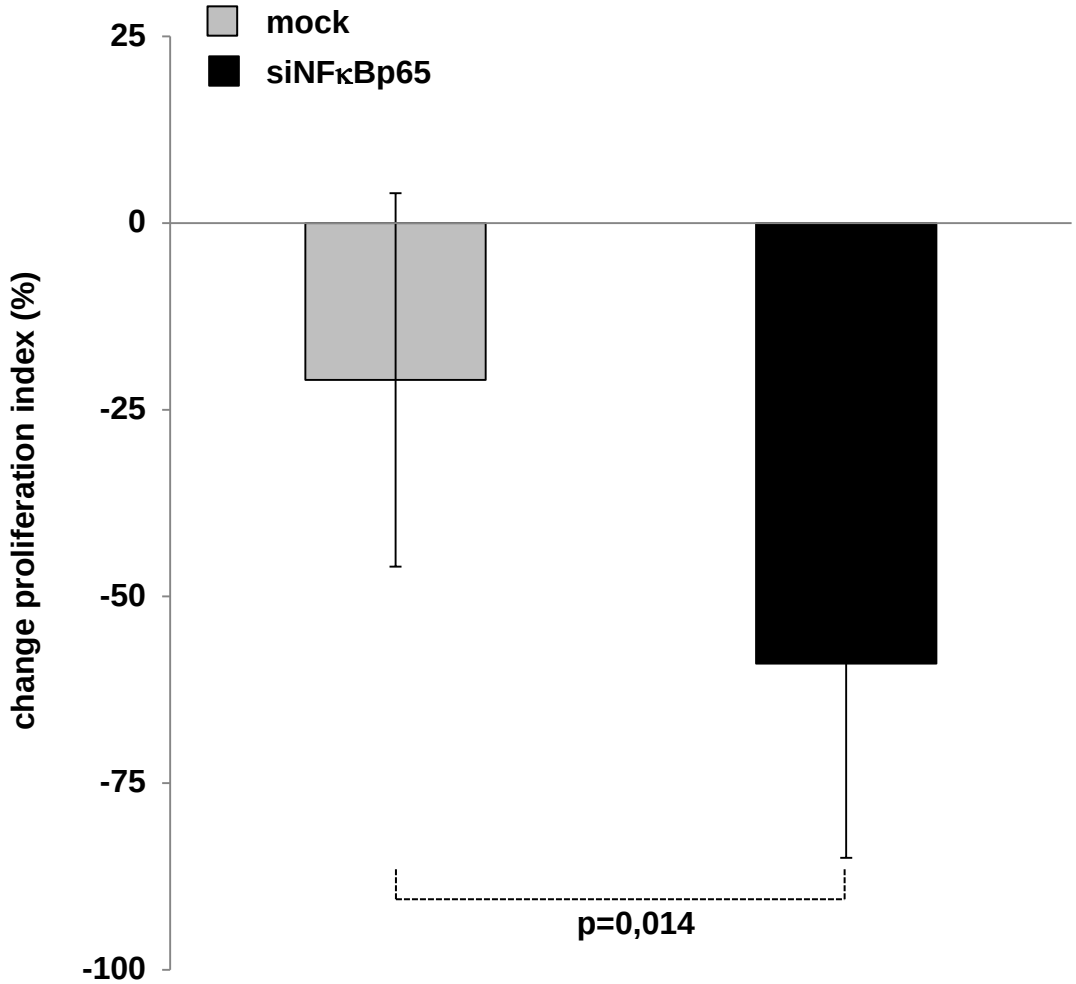

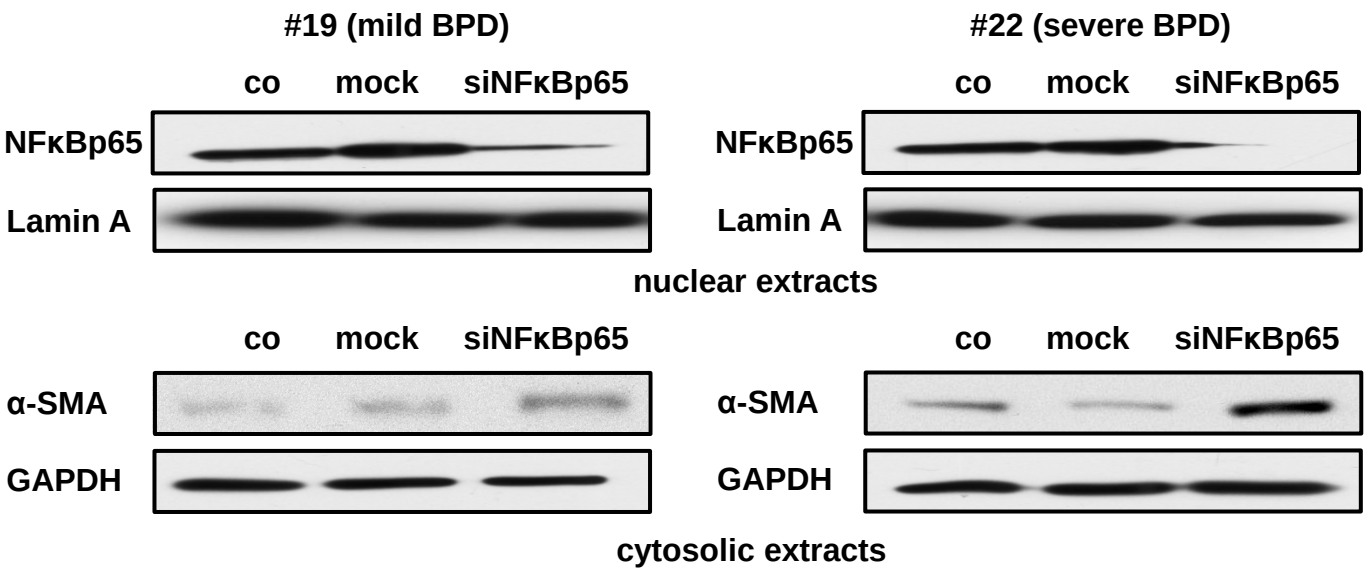

Figure 7

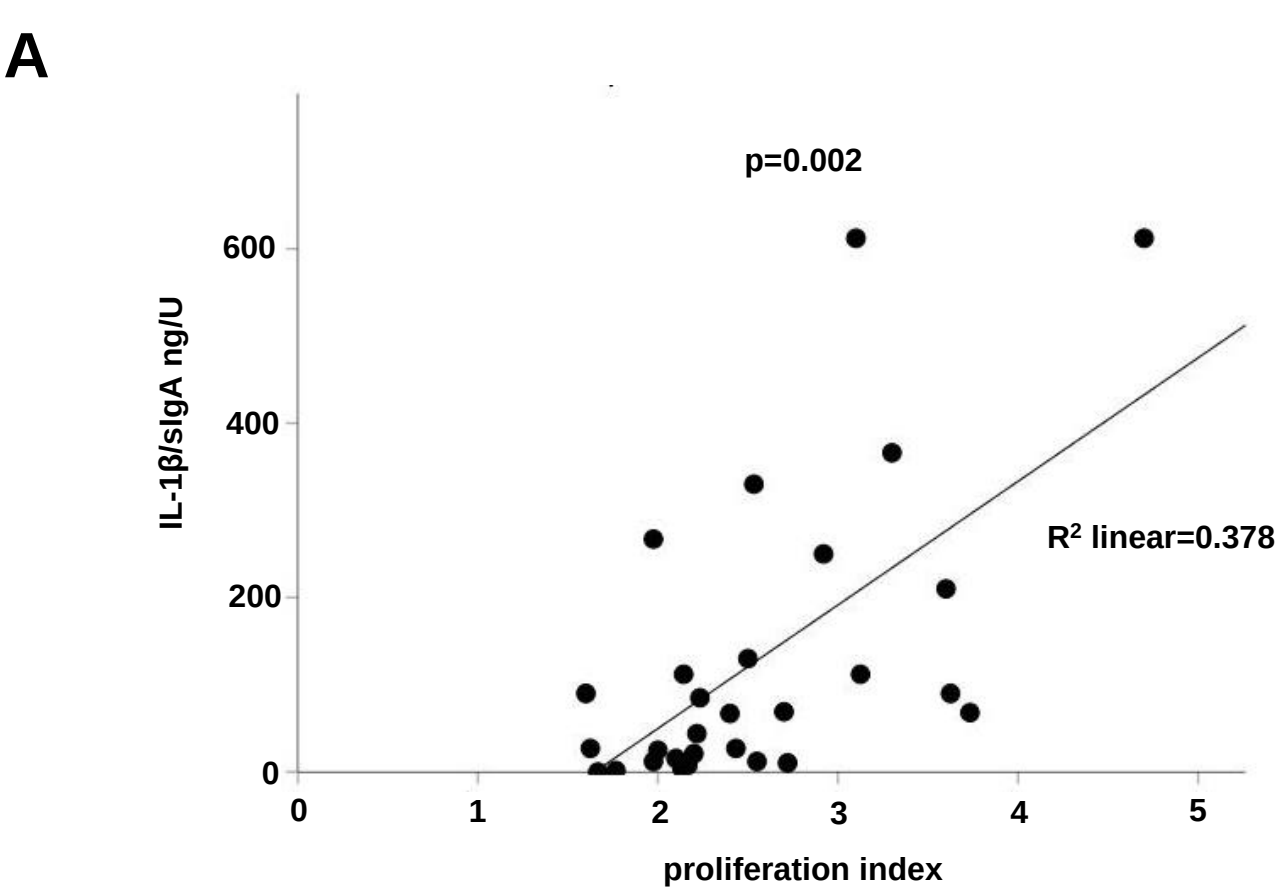

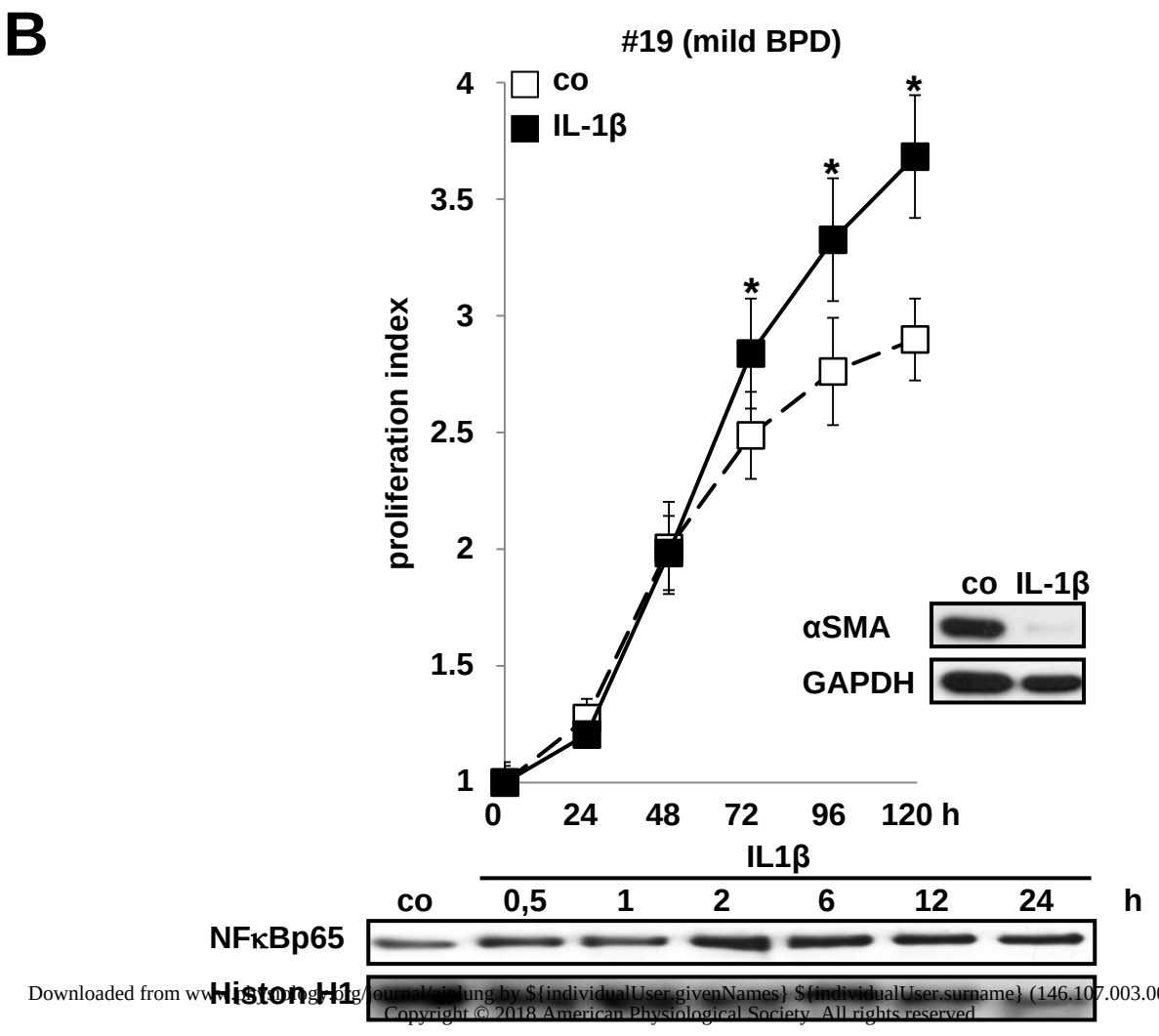

Figure 8

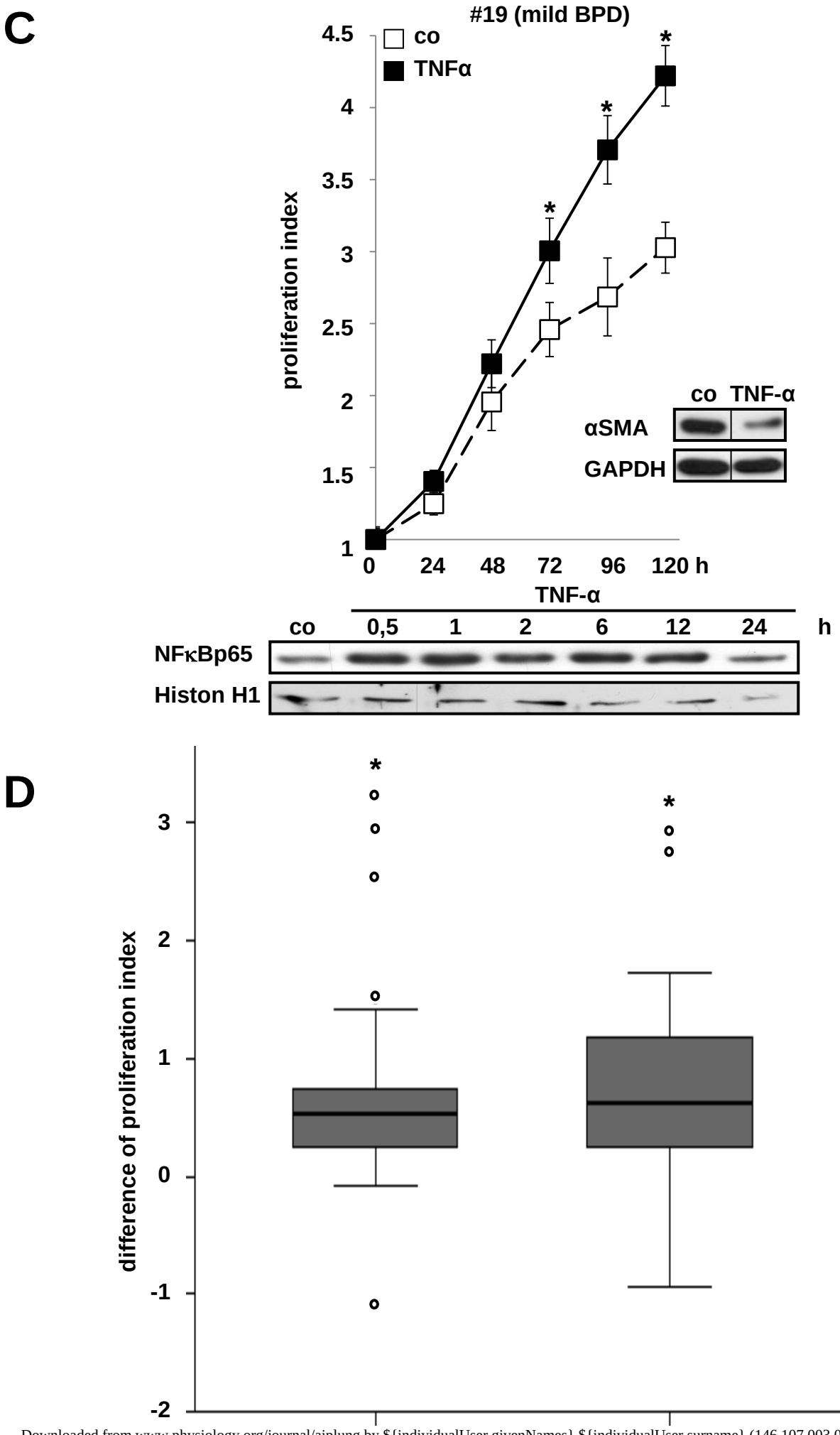

Figure 8

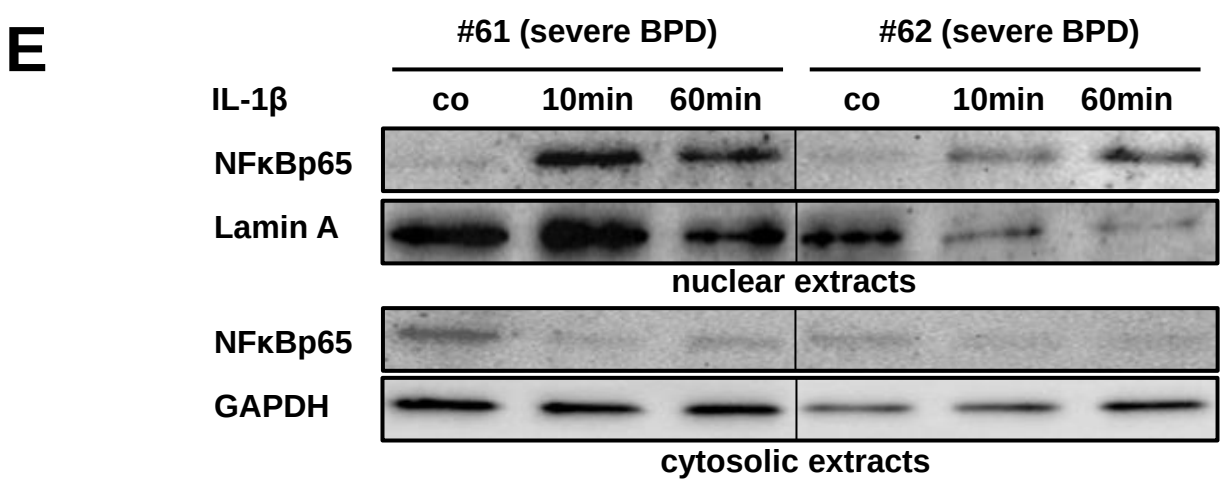

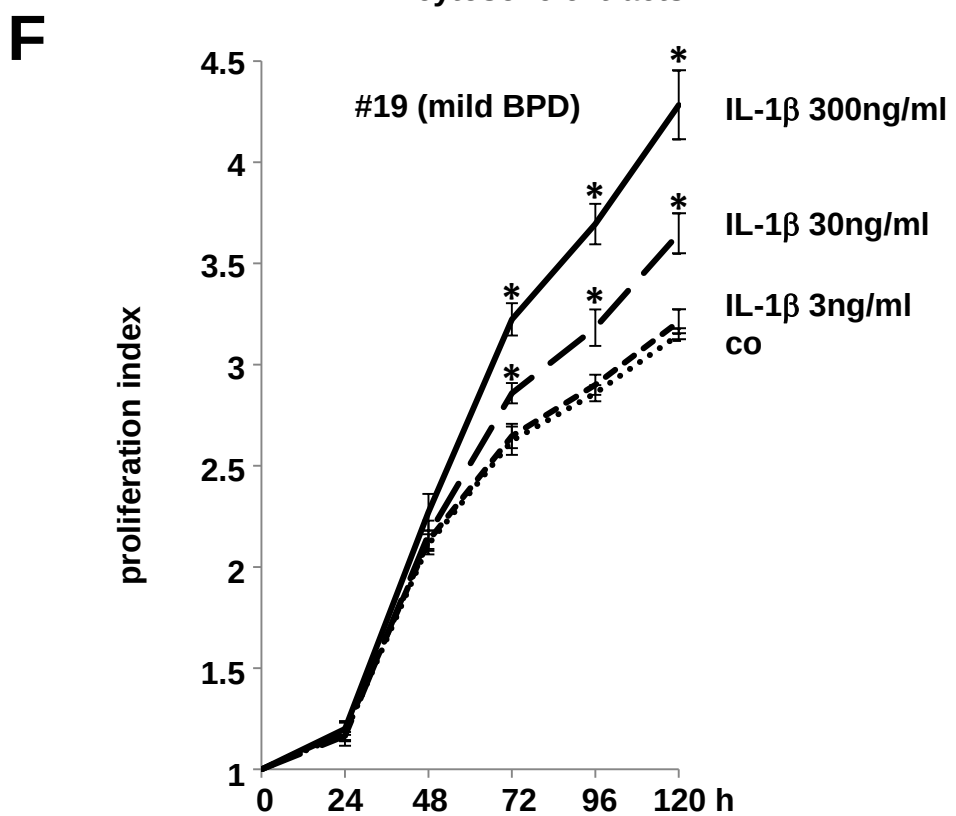

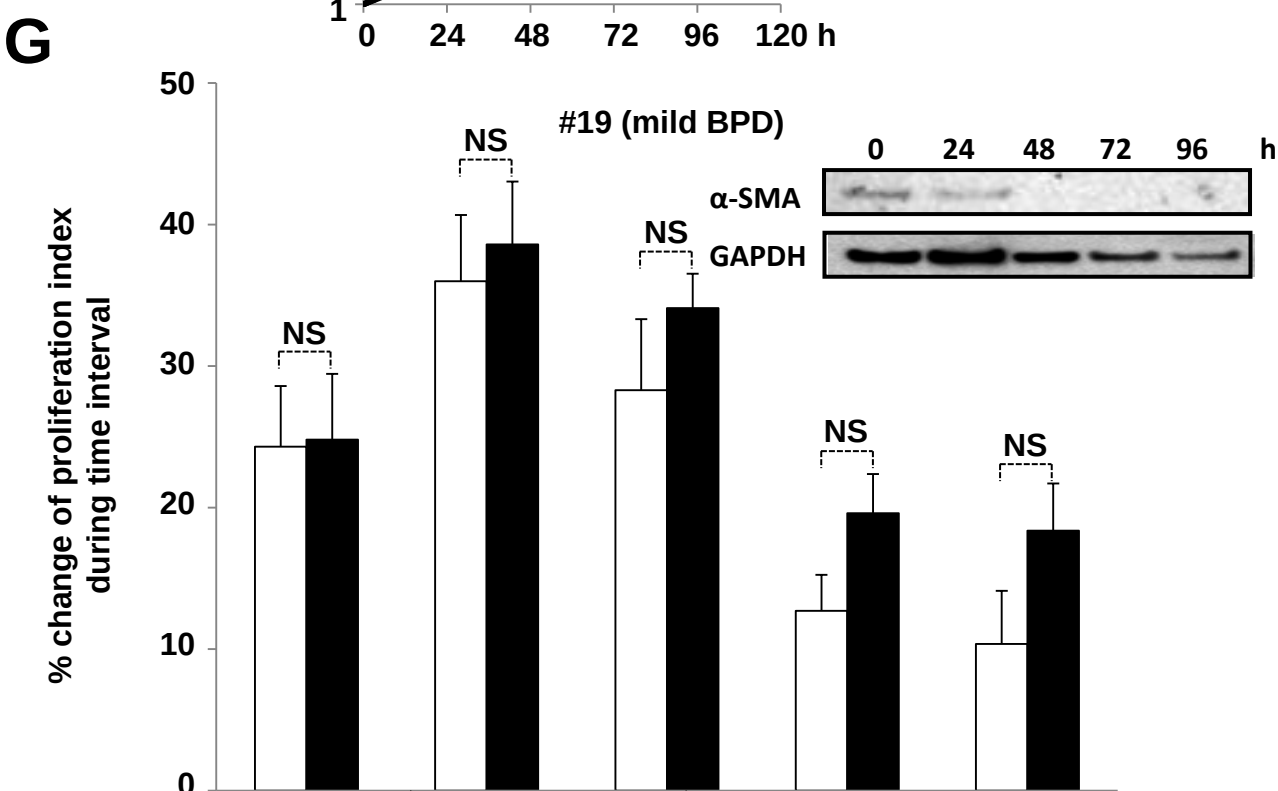

Figure 8

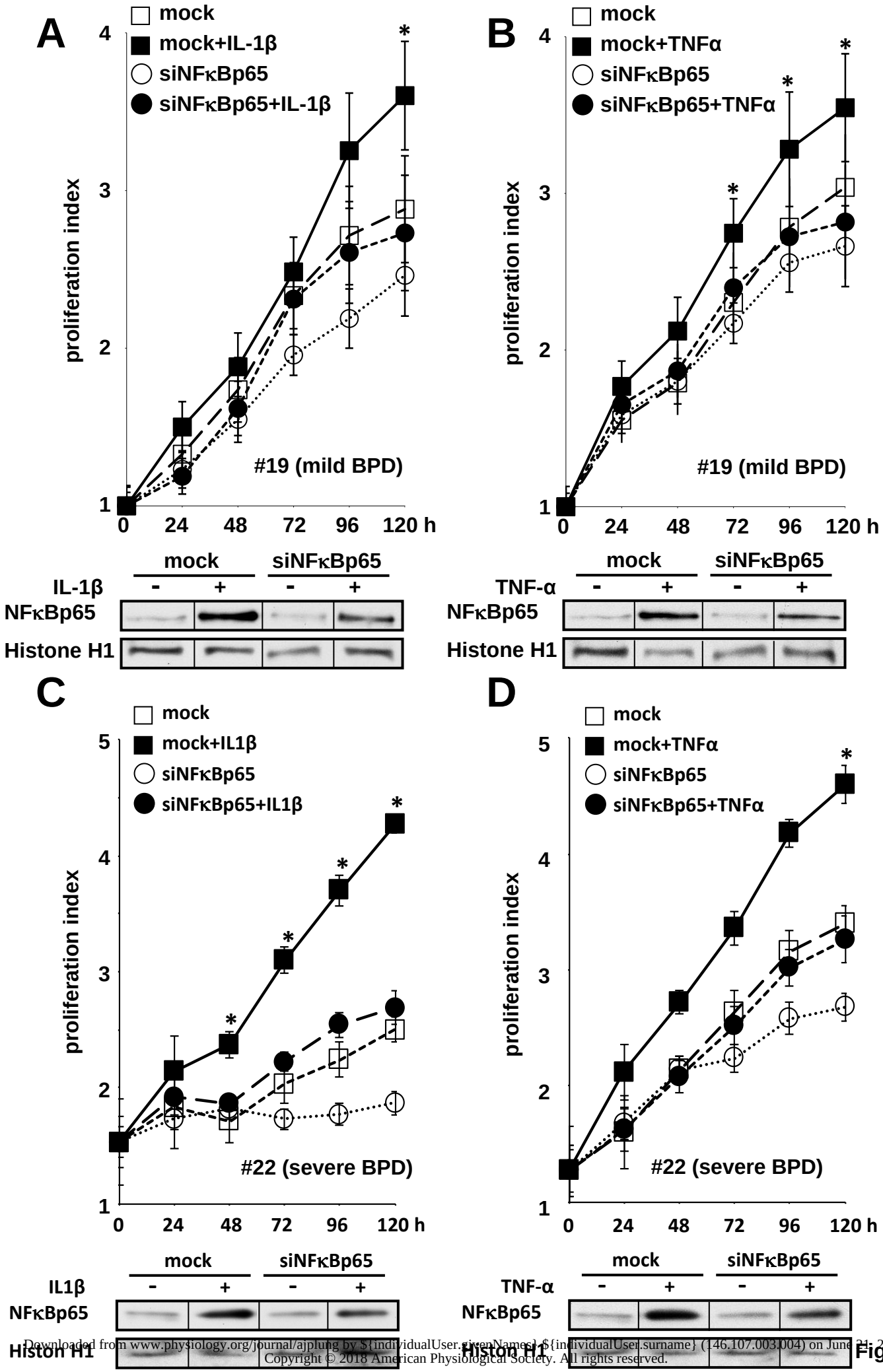

Figure 9